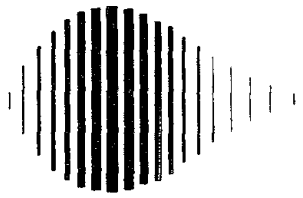

NATIONAL CENTER FOR EARTHQUAKE ENGINEERING RESEARCH

State University of New York at Buffalo

Experimental and Analytical Study of a Hybrid Isolation System Using Friction Controllable Sliding Bearings

by

M. Q. Feng and M. Shinozuka

Department of Civil Engineering and Operations Research
School of Engineering and Applied Sciences
Princeton University
Princeton, New Jersey 08544

and

S. Fujii

Technology Development Department
Technology Division
Taisei Corporation
Tokyo, Japan

Technical Report NCEER-92-0009

May 15, 1992

This research was conducted at Princeton University and Taisei Corporation and was partially supported by the National Science Foundation under Grant No. BCS 90-25010 and the New York State Science and Technology Foundation under Grant No. NEC-91029.

NOTICE

This report was prepared by Princeton University and Taisei Corporation as a result of research sponsored by the National Center for Earthquake Engineering Research (NCEER) through grants from the National Science Foundation, the New York State Science and Technology Foundation, and other sponsors. Neither NCEER, associates of NCEER, its sponsors, Princeton University, Taisei Corporation, nor any person acting on their behalf:

a. makes any warranty, express or implied, with respect to the use of any information, apparatus, method, or process disclosed in this report or that such use may not infringe upon privately owned rights; or

b. assumes any liabilities of whatsoever kind with respect to the use of, or the damage resulting from the use of, any information, apparatus, method or process disclosed in this report.

Any opinions, findings, and conclusions or recommendations expressed in this publication are those of the author(s) and do not necessarily reflect the views of the National Science Foundation, the New York State Science and Technology Foundation, or other sponsors.

Experimental and Analytical Study of a Hybrid Isolation System Using Friction Controllable Sliding Bearings

by

M.Q. Feng[1], S. Fujii[2] and M. Shinozuka[3]

May 15, 1992

Technical Report NCEER-92-0009

NCEER Project Number 90-2204

NSF Master Contract Number BCS 90-25010
and
NYSSTF Grant Number NEC-91029

1 Assistant Professor, University of California at Irvine; Former Research Assistant, Department of Civil Engineering and Operations Research, Princeton University
2 Manager, Technology Development Department, Taisei Corporation, Tokyo, Japan
3 Sollenberger Professor of Civil Engineering, Department of Civil Engineering and Operations Research, Princeton University

NATIONAL CENTER FOR EARTHQUAKE ENGINEERING RESEARCH
State University of New York at Buffalo
Red Jacket Quadrangle, Buffalo, NY 14261

PREFACE

The National Center for Earthquake Engineering Research (NCEER) was established to expand and disseminate knowledge about earthquakes, improve earthquake-resistant design, and implement seismic hazard mitigation procedures to minimize loss of lives and property. The emphasis is on structures in the eastern and central United States and lifelines throughout the country that are found in zones of low, moderate, and high seismicity.

NCEER's research and implementation plan in years six through ten (1991-1996) comprises four interlocked elements, as shown in the figure below. Element I, Basic Research, is carried out to support projects in the Applied Research area. Element II, Applied Research, is the major focus of work for years six through ten. Element III, Demonstration Projects, have been planned to support Applied Research projects, and will be either case studies or regional studies. Element IV, Implementation, will result from activity in the four Applied Research projects, and from Demonstration Projects.

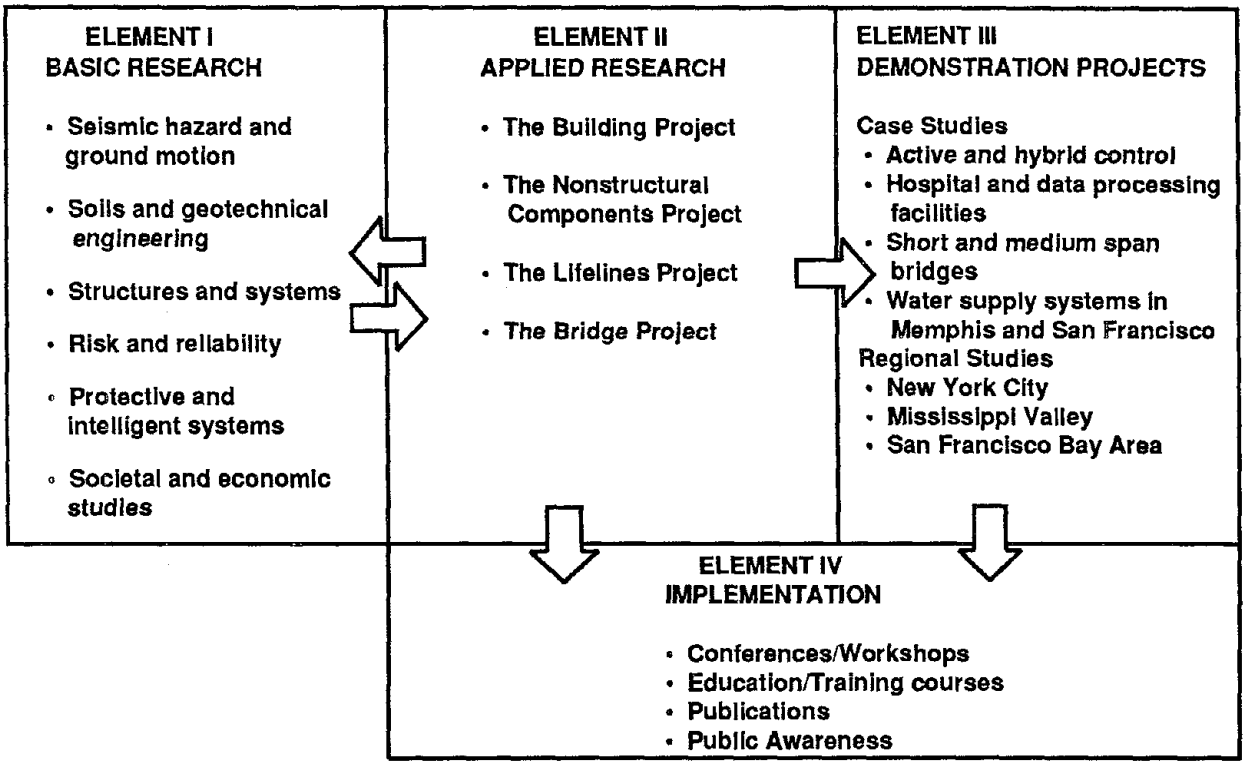

Research in the **Building Project** focuses on the evaluation and retrofit of buildings in regions of moderate seismicity. Emphasis is on lightly reinforced concrete buildings, steel semi-rigid frames, and masonry walls or infills. The research involves small- and medium-scale shake table tests and full-scale component tests at several institutions. In a parallel effort, analytical models and computer programs are being developed to aid in the prediction of the response of these buildings to various types of ground motion.

Two of the short-term products of the **Building Project** will be a monograph on the evaluation of lightly reinforced concrete buildings and a state-of-the-art report on unreinforced masonry.

The **protective and intelligent systems program** constitutes one of the important areas of research in the **Building Project**. Current tasks include the following:

1. Evaluate the performance of full-scale active bracing and active mass dampers already in place in terms of performance, power requirements, maintenance, reliability and cost.
2. Compare passive and active control strategies in terms of structural type, degree of effectiveness, cost and long-term reliability.
3. Perform fundamental studies of hybrid control.
4. Develop and test hybrid control systems.

This report describes the effectiveness of a hybrid isolation system using friction controllable sliding bearings. Two control algorithms, bang-bang control and instantaneous optimal control, are developed to control the friction force. Their effectiveness is demonstrated by shaking table experiments and computer simulation.

The hybrid sliding isolation system using friction controllable bearings is physically developed. Shaking table experiments are performed using a structural model equipped with the hybrid system. These experiments demonstrate the advantage of using the hybrid system over the passive system.

Computer codes to simulate the structural response under passive and hybrid control are developed. The numerically simulated results show good agreement with the experimental results. These results verify that the analytical model developed adequately represents the actual system.

ABSTRACT

This study deals with a hybrid isolation system using friction controllable sliding bearings [1,2]. During earthquakes, this isolation system controls the friction force on the sliding interface between the supported structure and the ground, by adjusting the pressure in a bearing chamber, to confine the sliding displacement within an acceptable range, while keeping the transfer of seismic force to a minimum to obtain the best isolation performance. This is the advantage of the hybrid sliding isolation system that cannot be achieved by the passive sliding system.

Instantaneous optimal control and bang-bang control algorithms are developed for controlling the friction force, since standard control theory is difficult to apply in a straightforward fashion in this case where the control force has a nonlinear feature. The effectiveness of the algorithms in controlling seismic response of a structural model is demonstrated by shaking table experiments and computer simulation.

A hybrid sliding isolation system using friction controllable bearings is physically developed, and shaking table experiments are performed using a rigid structural model equipped with such a hybrid system. The dynamic characteristics of the control system for bearing pressure and sliding friction is identified, and the advantage of the hybrid sliding isolation system over the passive system is demonstrated by experiments.

Computer codes for simulation of structural response under passive or hybrid control are developed. The numerically simulated results show good agreement with the experimental results, verifying that the analytical model developed represents the actual system very well.

Both experimental and analytical studies demonstrate the effectiveness of the hybrid sliding isolation system and suggest its advantageous use in civil structures.

ACKNOWLEDGEMENT

The authors wish to acknowledge the advice and encouragement provided by Professor T. Fujita of the University of Tokyo. This work was supported partially by the National Center for Earthquake Engineering Research under Grant Number NCEER 90-2204, and partially by Taisei Corporation, Tokyo, Japan.

Contents

List of Figures

List of Tables

SECTION 1

INTRODUCTION

1.1 Background

Seismic base isolation techniques have been used with increasing popularity to protect the structures, together with their occupants, secondary systems and internal equipment, from the damaging effects of earthquakes. The sliding isolation systems, however, have the following problems:

1. A structure supported entirely by sliding bearings experiences forces at the sliding interface that are always bounded by the frictional force, regardless of the intensity and frequency content of the ground excitation. From this view point, the smaller the coefficient, the higher the isolation performance. However, because of unavoidable residual displacement and possibly excessive sliding displacement associated with such systems, particularly those with small coefficients of friction, the purely sliding isolation system is difficult to use.

2. For practice, most of the sliding isolation systems currently in use are equipped with some form of restoring devices [3, 4, 5]. For a passive sliding system with a restoring force, the design of coefficient of friction and stiffness of the restoring device is not a simple problem. If the coefficient of friction is relatively small, then the isolation performance is greatly influenced by the stiffness of the restoring device. As a result, the advantage of the purely sliding isolation system (mentioned above) cannot be realized. For this reason, the coefficient of friction μ is usually designed to the extent (e.g., $\mu = 0.15 \sim 0.20$) that its isolation performance is not unduly influenced by the stiffness of the restoring device [6, 7]. However such a system becomes totally ineffective for the earthquakes with peak ground acceleration less than or equal to μg, in spite of the fact that such small to medium earthquakes occur more often and they can cause damage to sensitive equipment, valuable items and secondary systems inside the building.

3. Since a passive sliding isolation system is usually designed and effective for large earthquakes with long return periods, the system seldom has the opportunity to be activated during the service life of the building. For example, the TASS system (Kawamura et al. 1988) was installed in an office building (called J Building) in Yokohama, Japan four years ago, but has never been activated, although many small earthquakes occurred in that area during this period. Whether or not the sliding system can maintain the initially designed value of coefficient of friction throughout the long period of inactivity remains to be an important practical problem.

1.2 Objectives and Hybrid Isolation System

The objectives of this research are then to physically develop a friction controllable sliding isolation system which can retain the advantages, while eliminating the disadvantages, of the purely sliding isolation system, and thus delivers a fundamentally superior isolation performance which cannot be achieved by the passive sliding isolation system (with a restoring device).

To be more specific, this system can intelligently control the friction force on the sliding interface between the supported structure and the ground so as to confine the sliding displacement in an acceptable range, to reduce the residual displacement, and at the same time, to minimize the transfer of seismic force to the structure. For small to medium earthquakes, the friction force can be controlled to a small level to obtain the best isolation performance. For large earthquakes, the sliding displacement can be confined within an acceptable range by controlling the friction force, while the minimum isolation performance is guaranteed by the maximum friction force of the system. Therefore, this friction controllable sliding isolation system is effective for all intensities of earthquakes, (ranging from small, medium or large), unlike the passive sliding isolation systems which are usually designed for large earthquakes.

Furthermore, the confidence in this system can be more easily established than the passive sliding isolation system for the reason that this system has more opportunities of getting activated even under small earthquakes which occur more frequently.

To achieve these objectives, this research attempts to:

1. propose and physically develop a friction controllable sliding bearing and a hybrid sliding isolation system using such bearings,

2. develop control algorithms for controlling the friction force which has nonlinear characteristics,

3. through experiments and computer simulation analysis, demonstrate the effectiveness of the hybrid isolation system using friction controllable sliding bearings in controlling the seismic responses of both a single-degree-of-freedom structural model and a multi-degree-of-freedom building.

The hybrid isolation system using friction controllable bearings (FCB's) to be investigated is conceptually depicted in Figs. 1.1 and 1.2, respectively with a building and a bridge structure resting on the bearings. Each bearing has a fluid chamber which is connected to a pressure control system composed of a servo valve, an accumulator and a computer. The friction on the interface between the bearing and the ground is controlled by adjusting the fluid pressure in the chamber. The computer calculates an appropriate signal to control the fluid pressure based on the observed structural response, such as response acceleration and sliding displacement, and sends it to the pressure control device as shown in Figs. 1.1 and 1.2.

The idealized section view of the friction controllable sliding bearing is given in Fig. 1.3. The bearing made of steel is of disk shape containing a fluid chamber inside which is sealed by a rubber O-ring around the circular perimeter just inside the sliding interface. A sliding material such as PTFE plate is placed on the sliding surface.

The word "HYBRID" is used for this friction controllable sliding isolation system, since it is a combination of the passive sliding isolation system and the active control device. The system can be a passive sliding isolation system as long as the pressure of the bearing chamber, and thus the friction is kept at a constant value. At the same time, the system can

be an active system as long as the pressure is controlled so that the friction is controlled.

In the analytical formulation involving such a hybrid system, the control force does not appear in the equation of motion as an independent term like the force from an actuator. The active control in this case is implemented through the friction term in the equation, and in that sense the system may also be interpreted as "Semi-Active".

This hybrid isolation system has the following general advantages: (a) Changing friction force through controlling pressure requires smaller amounts of energy and power than the corresponding actuator-driven control system, and as a consequence (b), the use of accumulators for the source of energy is possible, thus eliminating the necessity of emergency energy supply system.

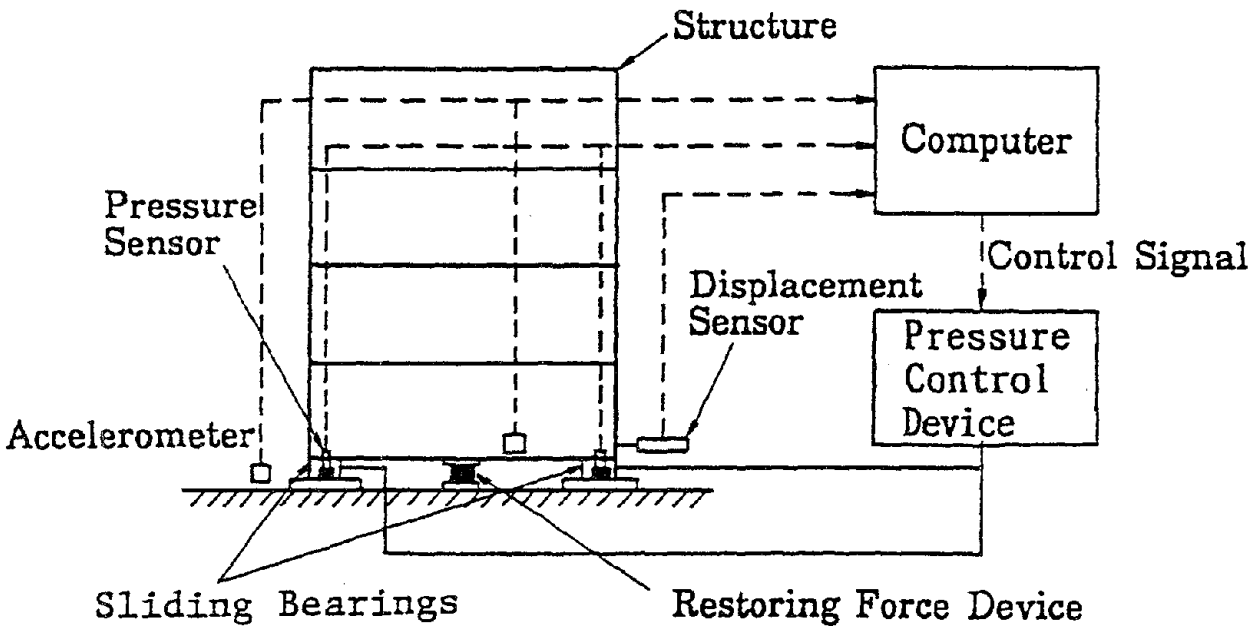

Figure 1.1: Concept of Hybrid Sliding Isolation System for Buildings

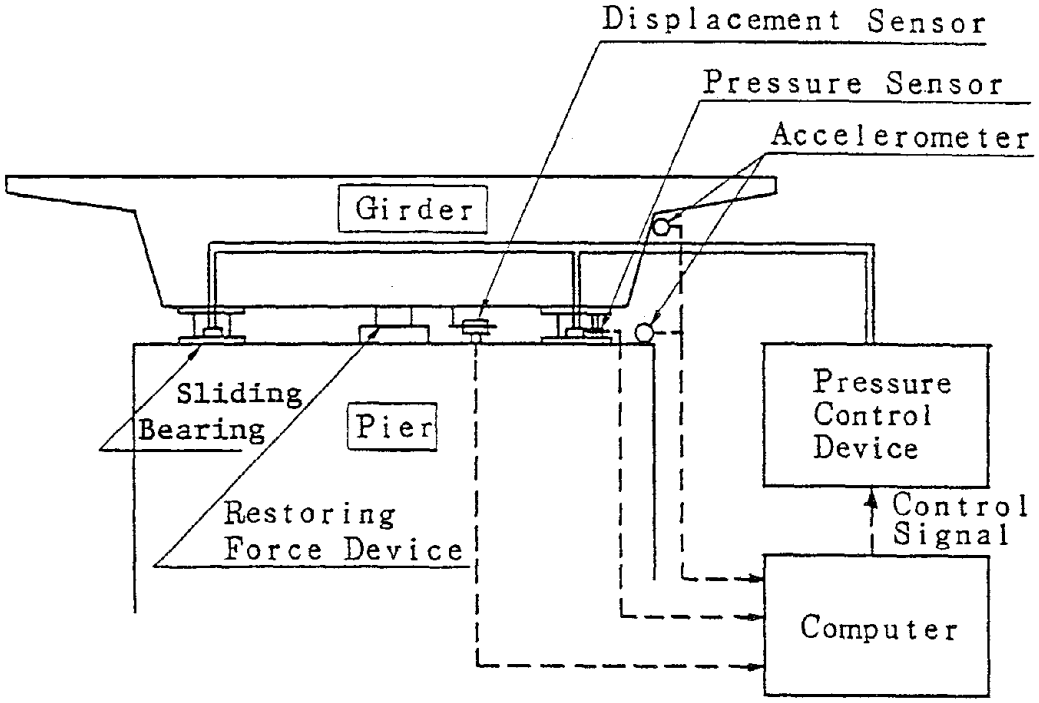

Figure 1.2: Concept of Hybrid Sliding Isolation System for Bridges

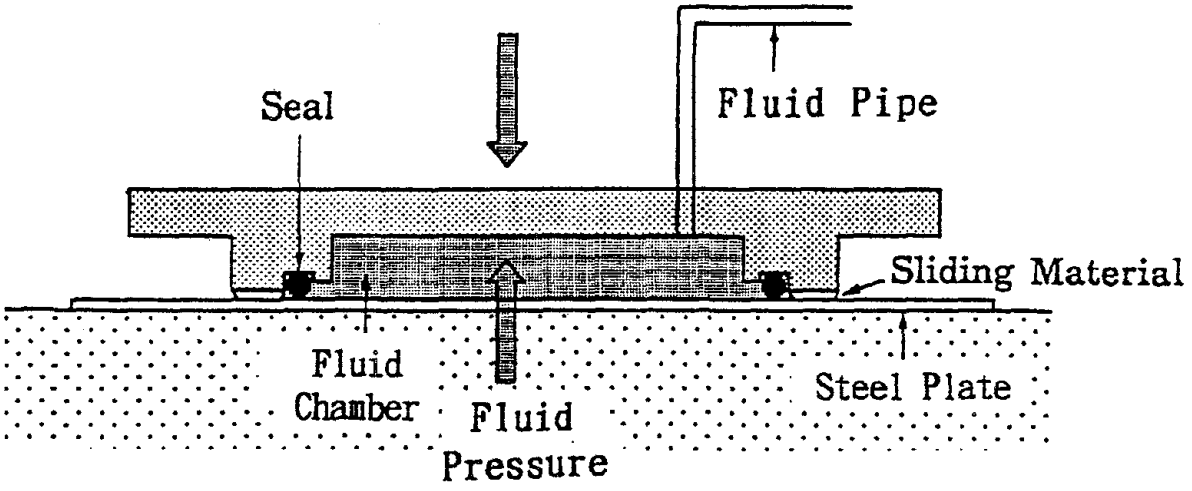

Figure 1.3: Idealized View of Friction Controllable Sliding Bearing

1.3 Outline of the Study

In Section 2, two kinds of control algorithms are newly developed for controlling the friction force in the sliding isolation system, since standard control theory can not be applied in a straightforward fashion in this case where the analytical model of the physical system is nonlinear involving the friction force. These control algorithms are either based on instantaneous optimal control theory or bang-bang control method. As to the instantaneous optimal control, two cases are studied: one takes into account the time delay of the friction control system, while the other does not. These control algorithms, whether based on instantaneous optimal control or bang-bang control, are relatively simple and yet robust for on-line control operations, and they effectively achieve the objectives mentioned above.

In Sections 3 and 4, the experimental study performed on a single-degree-of-freedom structure installed with a hybrid sliding isolation system is described. The sliding bearing and its control device are developed. A single-degree-of-freedom model structure is constructed. Computer codes using the C language for real-time on-line control operations are developed. The characteristics of the hybrid isolation system is identified by experiments. Then, the hybrid isolation system which can control the friction force in the sliding interface between the model structure and the ground (shaking table) is developed. It can act as a passive isolation system by maintaining the friction force at a certain value. Shaking table experiments of the model structure equipped with such a sliding isolation systems are carried out to evaluate its isolation performance under various earthquake excitations with differing levels of intensities. The isolation performance of the hybrid system is compared with that of the passive system, and the advantage of the proposed hybrid sliding isolation system is demonstrated.

In Section 5, related analytical and numerical studies also performed. A computer pro-

gram for numerical evaluation of the response of the structure under passive or hybrid isolation is developed. The numerical simulation results show a good agreement with the experimental results, confirming the adequacy of the analytical model and the simulation method.

Finally, the conclusion of this report is given in Section 6.

SECTION 2

CONTROL ALGORITHMS

Control of structural response by the proposed hybrid sliding isolation system using friction controllable bearings presents an unique problem in developing control algorithms. The reason is that the control force in this sliding isolation system is the friction force, which depends on the direction of the sliding velocity and thus appears as a nonlinear term in the equation of motion. For controlling such a nonlinear force, standard control theory is difficult to apply, and not much research has been done to derive control algorithms. Fujita et al [8, 9] developed a semi-active seismic isolation system using controllable friction dampers. In this system, the frictional damping force is controlled by changing the pressure between the friction elements using an actuator. Linear optimal control algorithm in modern control theory was applied in a straightforward manner in this study. Since the frictional damping force is a nonlinear force depending on the direction of velocity, the optimal control force required by the linear control theory cannot be fully realized by the friction force, and thus the real "optimal control" can not be implemented. In this respect, Feng and Shinozuka [10, 11] were the first to derive a nonlinear control alorithm on the basis of instantaneous optimal

control [12, 13] for the system with such a nonlinear control force. By simulation study, they showed the effectiveness of the control algrithm. In their study, however, nonlinear differential equations are needed to be solved for control force at every control time instant, making real-time on-line control operations rather difficult.

In this study, two types of control algorithms, both of which are implementable in real-time on-line operations, are developed to control the nonlinear friction force in the proposed hybrid isolation system under earthquake loads. They are developed on the basis of the instantaneous optimal control thcory and bang-bang control concept. As to the instantaneous optimal control, furthermore, two cases are studied: one with the time delay of the friction control system taken into consideration and the other without.

2.1 Analytical Model

A rigid structure supported by the friction controllable sliding bearings is considered. The motion of the structure can be modeled by a single-degree-of-freedom (SDOF) model as shown in Fig. 2.1. The equations of motion of the structure under earthquake excitation can then be written as follows.

1. Sticking Phase — Phase I

$$\dot{x} = 0, \quad x = const. \tag{2.1}$$

2. Sliding Phase — Phase II

$$\ddot{x} = -\ddot{z} - f \ \mathrm{sgn}(\dot{x}), \tag{2.2}$$

3. Criteria for transition from Phase I to Phase II

$$|\ddot{z}| > f \tag{2.3}$$

4. Criteria for transition from Phase II to Phase I

$$\dot{x} = 0 \tag{2.4}$$

$$|\ddot{x}| < 2f \tag{2.5}$$

where

x: sliding displacement of mass relative to ground

$\ddot{z}$: input earthquake acceleration

μ: coefficient of friction on sliding interface

f: normalized friction force defined as $f = \mu g$

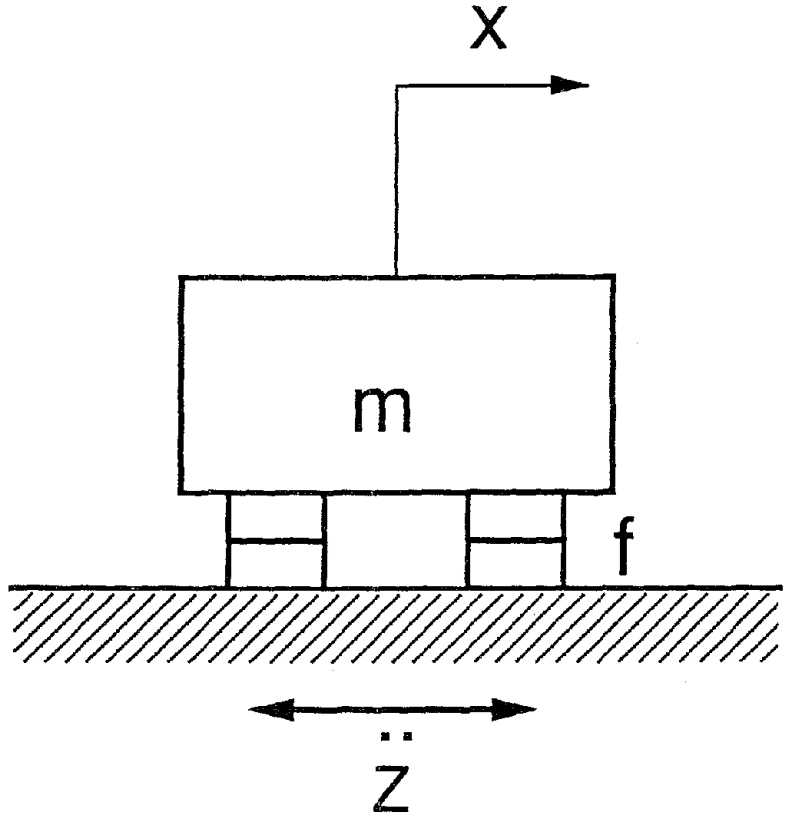

Figure 2.1: Analytical Model

In the sticking phase, Eq. 2.1 governs the motion of the structure until the Eq. 2.3 becomes true. As soon as the condition in Eq. 2.3 is met, the sliding phase starts and Eq. 2.2 governs the sliding motion. During the sliding phase, whenever $\dot{x}$ becomes zero, the criterion, Eq. 2.4, is checked to determine the subsequent behavior. Validity of the inequality given by Eq. 2.4 is the condition for entering the sticking phase [14]. That is, if the inequality holds, the structure will stick to the ground and Eq. 2.1 applies. If the criterion given by Eq. 2.4 is not satisfied, Eq. 2.1 will continue to govern the the subsequent sliding motion.

On the other hand, the normalized friction force f on the sliding interface between the structure and the ground is controlled by changing the fluid pressure in the bearing chamber through a pressure control system consisting of a computer, servo valve, amplifier, etc. The dynamic characteristics of the pressure control system are assumed to follow the first order time delay model:

$$T\dot{p} + p = u \tag{2.6}$$

where

p: pressure in fluid chamber of bearing

u: pressure control signal from computer

T: time constant

The normalized friction force f is negatively proportional to the pressure p in the bearing chamber:

$$f = -c_1 p + c_2 \tag{2.7}$$

where c_1 and c_2 are constants.

2.2 Bang-Bang Control

Bang-bang control approach provides a simple and yet often effective algorithm. The particular algorithm used in this study facilitates the following control: when the sliding displacement and the velocity of the mass are in the same direction, the pressure control signal $u(t)$ will be decreased to a minimum value u_{min} to increase the friction force in order to put the brake on the sliding. On the other hand, when the sliding displacement and the velocity are in the opposite direction, the pressure control signal will be increased to a maximum value u_{max} to decrease the friction force in order to make the sliding easier as much as possible;

$$u(t) = \begin{cases} u_{max}, & \text{if } \mathrm{sgn}(x) = -\mathrm{sgn}(\dot{x}) \\ u_{min}, & \text{if } \mathrm{sgn}(x) = \mathrm{sgn}(\dot{x}) \end{cases} \tag{2.8}$$

in which the control parameter, u_{max} and u_{min}, should be determined carefully, since they directly influence the control performance.

u_{max} should be set at a level as large as possible in order to reduce the friction force to a minimum level, making the mass slide as much as possible. It is, however, limited by the maximum pressure which can be applied to the bearing chamber. This depends on the weight W of the structure supported by the bearing:

$$u_{max} < \frac{W}{S} \tag{2.9}$$

where S is the vertically projected area of the fluid chamber of bearing. u_{min} should be set at a small level in order to confine the sliding displacement within an acceptable range.

This bang-bang control algorithm is simple and easy to implement in real-time on-line control operations, since the control signal only switches between two values, and only the sliding displacement needs to be measured by a sensor and fed back to the control signal.

Notice that $\mathrm{sgn}(\dot{x})$ can be obtained by the displacement signal and does not need to measure the velociy

However, this algorithm has the following difficulty: In order to confine the sliding displacement within an acceptable range, the smaller value of u_{min} is needed. The smaller u_{min}, however, will lead to the larger seismic response acceleration of the structure and thus degrade the isolation performance. This conflict can only be alleviated, it appears, by taking advantage of pertinent optimal control algorithms.

2.3 Instantaneous Optimal Control

2.3.1 Formulation

As mentioned earlier, control theory has not been well developed for such systems in which the control force has the nonlinearity, unique to the friction controllable sliding isolation device. For this reason, an optimal control algorithm for control of the nonlinear friction system is developed on the basis of the instantaneous optimal control theory originally proposed by Yang et al. [12, 13].

The optimal pressure control signal $u(t)$ is determined by minimizing the following time dependent objective function $J(t)$ at every time instant t for the entire duration of an earthquake.

$$J(t) = q_d x^2(t) + q_f f^2(t) + r u^2(t) \tag{2.10}$$

in which the normalized friction force f equivalently represents the amount of response acceleration and also serves as a measure of the transfer of seismic force to the structure. The weighting coefficient q_d and q_f are non-negative and r is positive. They indicate the relative importance in the control objectives of the sliding displacement, response acceleration and pressure control signal, respectively. The basic objectives of the control is to make the structure slide as much as possible within an acceptable range and at the same time to ensure the transfer of seismic force to a minimum.

The following control algorithm is derived under the assumption that the structural motion is always in the sliding phase. The equation of motion given by Eq. 2.2 should be used as a constraint when minimizing the objective function $J(t)$. The first order time delay relationship between the control signal and the pressure described in Eq. 2.6, as well

as the linear relationship between the friction and the pressure shown in Eq. 2.7, are also constraints. In the present formulation, however, these equations will be solved numerically using the Newmark's β method with $\beta = 1/6$ as shown below and these numerical solutions will be used as constraints:

$$\Delta\dot{x}(t) = \ddot{x}(t)\ \Delta t + \Delta\ddot{x}(t)\ \frac{\Delta t}{2} \tag{2.11}$$

$$\Delta x(t) = \dot{x}(t)\ \Delta t + \ddot{x}(t)\ \frac{\Delta t^2}{2} + \Delta\ddot{x}(t)\ \frac{\Delta t^2}{6} \tag{2.12}$$

$$\Delta f(t) = \dot{f}(t)\ \Delta t + \Delta\dot{f}(t)\ \frac{\Delta t}{2} \tag{2.13}$$

From the above equations, one obtains:

$$x(t) = x(t-\Delta t) + \dot{x}(t-\Delta t)\ \Delta t + \ddot{x}(t-\Delta t)\frac{\Delta t^2}{2} + [\ddot{x}(t) - \ddot{x}(t-\Delta t)]\frac{\Delta t^2}{6} \tag{2.14}$$

$$f(t) = f(t-\Delta t) + \dot{f}(t-\Delta t)\ \Delta t + [\dot{f}(t) - \dot{f}(t-\Delta t)]\frac{\Delta t}{2} \tag{2.15}$$

Furthermore,

$$x(t) = a\ f(t)\ \mathrm{sgn}(\dot{x}(t)) + b\ddot{z}(t) + d_1\ (t-\Delta t) \tag{2.16}$$

$$f(t) = -c\ u(t) + d_2(t-\Delta t) \tag{2.17}$$

where

$$a = b = -\frac{\Delta t^2}{6}, \qquad c = \frac{c_1 \Delta t}{2\ T + \Delta t} \tag{2.18}$$

$$d_1(t-\Delta t) = x(t-\Delta t) + \dot{x}(t-\Delta t)\Delta t + \frac{1}{3}\ \ddot{x}\ (t-\Delta t)\ \Delta t^2 \tag{2.19}$$

$$d_2(t-\Delta t) = \frac{2\ T}{2\ T + \Delta t}\left(\frac{c_2\ \Delta t}{2T} + f(t-\Delta t) + \frac{1}{2}\dot{f}(t-\Delta t)\Delta t\right) \tag{2.20}$$

The numerical solution to Eq. 2.2 given in Eq. 2.16, and the numerical solution to Eqs. 2.6 and 2.7 expressed in Eq. 2.17 are used as constraints as mentioned above. Thus,

the following generalized objective function is established by introducing the Lagrangian multipliers λ_1 and λ_2:

$$\begin{aligned} H(t) &= q_d\, x^2(t) + q_f\, f^2(t) + r\, u^2(t) \\ &\quad +\lambda_1 \left[x(t) - a\, f(t)\, \mathrm{sgn}(\dot{x}(t)) - b\, \ddot{z}(t) - d_1\, (t - \Delta t)\right] \\ &\quad +\lambda_2 \left[f(t) + c\, u(t) - d_2\, (t - \Delta t)\right] \end{aligned} \tag{2.21}$$

The necessary conditions for minimizing the objective function $J(t)$ are:

$$\frac{\partial H}{\partial x} = 0, \quad \frac{\partial H}{\partial f} = 0, \quad \frac{\partial H}{\partial u} = 0, \quad \frac{\partial H}{\partial \lambda_1} = 0, \quad \frac{\partial H}{\partial \lambda_2} = 0, \tag{2.22}$$

Substituting Eq. 2.21 into Eq. 2.22 yields the optimal pressure control signal:

$$u(t) = F_f\, f(t) + F_d\, x(t)\, \mathrm{sgn}(\dot{x}(t)) \tag{2.23}$$

where, the control feedback gains F_f and F_d are calculated by

$$F_f = \frac{c\, q_f}{r}, \quad F_d = \frac{c\, a\, q_d}{r} \tag{2.24}$$

and the displacement $x(t)$ and friction $f(t)$ are used for feedback purpose. Again, notice that $\mathrm{sgn}(\dot{x})$ can be obtained from the displacement signal without the need to measure the velocity. The friction is difficult to measure by a sensor, but the signal from the acceleration sensor $(\ddot{x}(t) + \ddot{z}(t))$ can be used instead of f in the SDOF structure. Therefore, the control signal becomes:

$$u(t) = F_f\, |\ddot{x}(t) + \ddot{z}(t)| + F_d\, x(t)\, \mathrm{sgn}(\dot{x}(t)) \tag{2.25}$$

In the development of the optimal control algorithm shown above, the time delay of the control device shown in Eq. 2.6 has been incorporated. In this case, the control is referred to as "instantaneous optimal control with time delay".

If the response of the control device is so fast that the time delay can be ignored, the relationship between the pressure and the control signal is given by:

$$p(t) = u(t) \tag{2.26}$$

The control algorithm is also developed under this condition, in which case the objective function and Hamiltonian become respectively:

$$J(t) = q_d x^2(t) + q_f f^2(t) + r\ u^2(t) \tag{2.27}$$

and

$$\begin{aligned} H(t) \;=\; & q_d\ x^2(t) + q_f\ f^2(t) + r\ u^2(t) \\ & +\lambda_1 \left[x(t) - a\ f(t)\ \mathrm{sgn}(\dot{x}(t)) - b\ \ddot{z}(t) - d_1\ (t - \Delta t)\right] \\ & +\lambda_2 \left[f(t) + c_1\ u(t) - c_2\right] \end{aligned} \tag{2.28}$$

The control based on Eq. 2.26 is referred to as "instantaneous optimal control without time delay". By letting the following partial derivatives equal to zero,

$$\frac{\partial H}{\partial x} = 0, \quad \frac{\partial H}{\partial f} = 0, \quad \frac{\partial H}{\partial u} = 0, \quad \frac{\partial H}{\partial \lambda_1} = 0, \quad \frac{\partial H}{\partial \lambda_2} = 0, \tag{2.29}$$

the following control signal is obtained:

$$u(t) = F + F_d\ x(t)\ \mathrm{sgn}(\dot{x}(t)) \tag{2.30}$$

where

$$F = \frac{c_1 c_2 q_f}{r + q_f {c_1}^2}, \quad F_d = \frac{c_1 a q_d}{r + q_f {c_1}^2} \tag{2.31}$$

In this case, only the sliding displacement $x(t)$ needs to be measured and fed back.

Such instantaneous optimal control algorithms are also applicable to deal with other types of nonlinearity, by establishing a time dependent objective function and using numerical solutions of nonlinear equations as constraints to minimize objective function.

2.3.2 Sufficient Condition For Optimal Control

In the original derivations for the instantaneous optimal control algorithms shown above, the optimal control signals $u(t)$ are obtained from the necessary conditions, such as Eq. 2.22 and Eq. 2.29. In fact, the derived optimal control signals $u(t)$ also satisfy the sufficient conditions of optimality as will be proved in the following.

The sufficient condition for the optimal solution shown in Eq. 2.23 is given by [15, 16]:

$$[\delta x \ \delta f \ \delta u] \begin{bmatrix} \frac{\partial^2 H}{\partial x^2} & \frac{\partial^2 H}{\partial x \partial f} & \frac{\partial^2 H}{\partial x \partial u} \\ \frac{\partial^2 H}{\partial f \partial x} & \frac{\partial^2 H}{\partial f^2} & \frac{\partial^2 H}{\partial f \partial u} \\ \frac{\partial^2 H}{\partial u \partial x} & \frac{\partial^2 H}{\partial u \partial f} & \frac{\partial^2 H}{\partial u^2} \end{bmatrix} \begin{bmatrix} \delta x \\ \delta f \\ \delta u \end{bmatrix} > 0 \tag{2.32}$$

Taking derivatives of H in Eq. 2.21 obtains:

$$\begin{gathered} \frac{\partial^2 H}{\partial x^2} = 2q_d, \qquad \frac{\partial^2 H}{\partial f^2} = 2q_f, \qquad \frac{\partial^2 H}{\partial u^2} = 2r, \\ \frac{\partial^2 H}{\partial x \partial f} = \frac{\partial^2 H}{\partial f \partial x} = 0, \quad \frac{\partial^2 H}{\partial x \partial u} = \frac{\partial^2 H}{\partial u \partial x} = 0, \quad \frac{\partial^2 H}{\partial f \partial u} = \frac{\partial^2 H}{\partial u \partial f} = 0 \end{gathered} \tag{2.33}$$

Substitution of Eq. 2.33 into the left hand side of Eq. 2.32 leads to the following expression:

$$2 \ [\ q_d \ (\partial x)^2 + q_f \ (\partial f)^2 + r \ (\partial u)^2 \ ] > 0 \tag{2.34}$$

which is true since q_d and q_f are non-negative and r is positive, Eq. 2.32 is greater than zero. Thus, the sufficient condition for the optimal solution, Eq. 2.32, is satisfied.

Similarly, it can be shown that the optimal signal derived under the condition of no time delay, Eq. 2.30, also satisfies the sufficient condition.

SECTION 3

SHAKING TABLE EXPERIMENT

In order to examine the performance of the proposed hybrid isolation system and to study the feasibility of its applications in structural engineering, experimental studies have been performed. For this purpose, a prototype hybrid isolation system with the friction controllable sliding bearings has been developed. A rigid structural model supported on the hybrid system was experimented on a shaking table at Taisei Technology Research Center in Yokohama, Japan. This three dimensional shaking table has a maximum stroke of 40 cm in each horizontal direction and maximum loading capacity of 20 tonf weight.

3.1 Structure Model and Isolation Device

The structure model used for experiments is shown in Fig. 3.1. The model, representing a rigid structure, consists of a steel frame and steel weights. The total weight of the model is 12 tonf.

Figures 3.2 and is a photograph of the structure model in the experiments. The model is supported equally by four friction controllable sliding bearings on the shaking table, as

shown in Figs. 3.1 and 3.2. The bearing developed for the experiments is shown in Fig. 3.3 and Fig. 3.4. Figure 3.5 is a photograph of the bearing being used in the experiments. The bearing, with a brass sheet of 1 mm thickness attached to be used as sliding surface, slides on a stainless steel plate fixed on steel I-bars bolted down on the shaking table, as shown in Figs. 3.1 and 3.2. Furthermore, a rubber O-ring of 5.7 mm in diameter acts as seal for the fluid in the fluid chamber. The area of the sliding surface is 86.0 cm^2, and the vertically projected area of the fluid chamber is 57.7 cm^2. No restoring force device is used in order to study the effect of friction force only. A servo valve is located at the center of the experimental structure from which the pressurized fluid is distributed to each sliding bearing as described in Fig. 3.1.

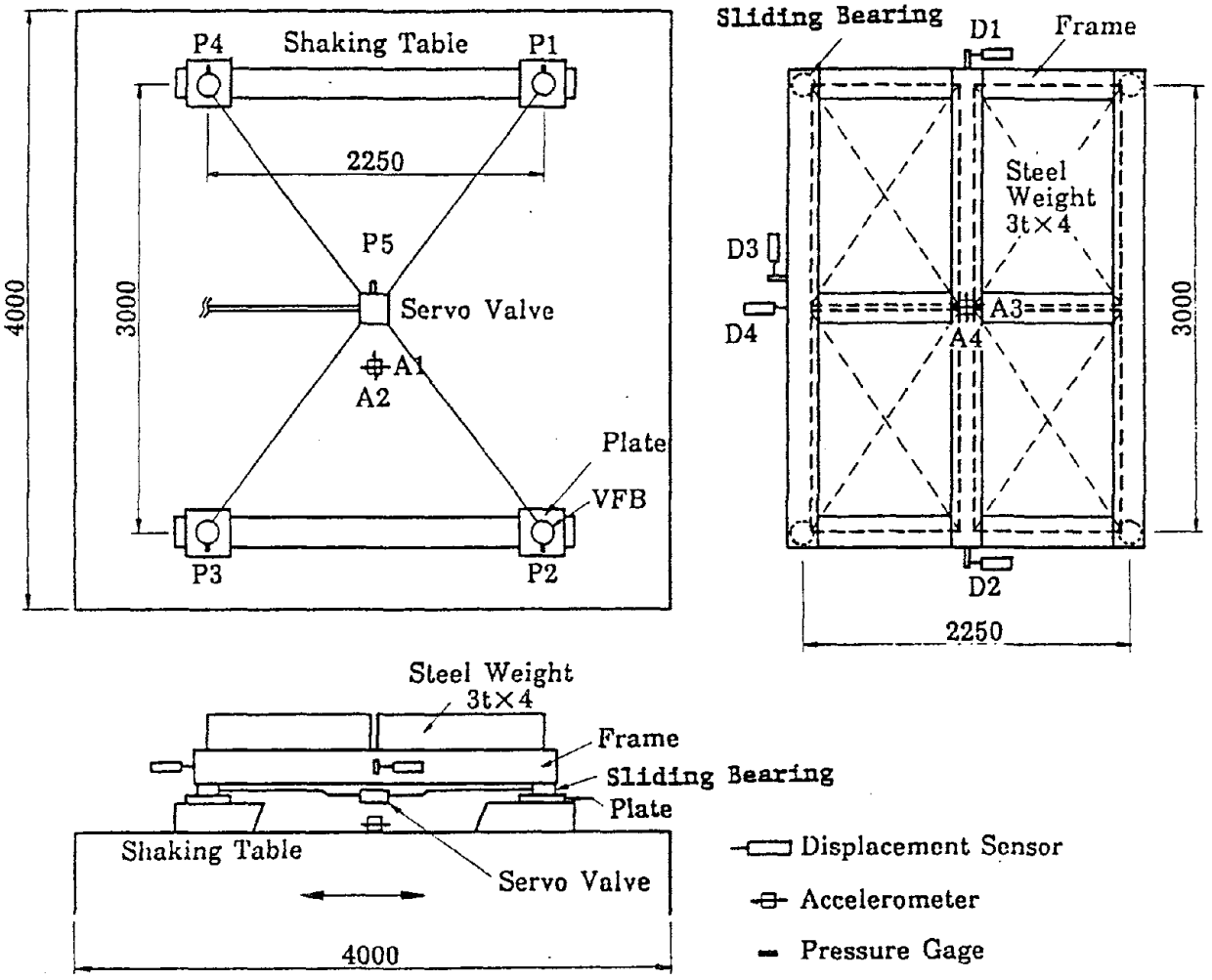

Figure 3.1: Structure Model with Hybrid Sliding Isolation Device

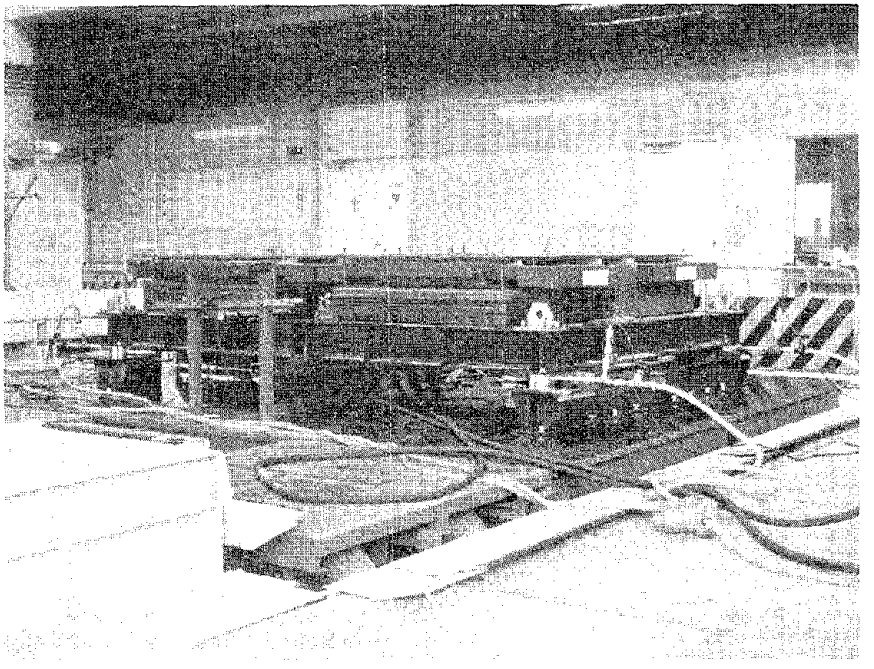

Figure 3.2: Structure Model with Hybrid Sliding Isolation Device in Experiment

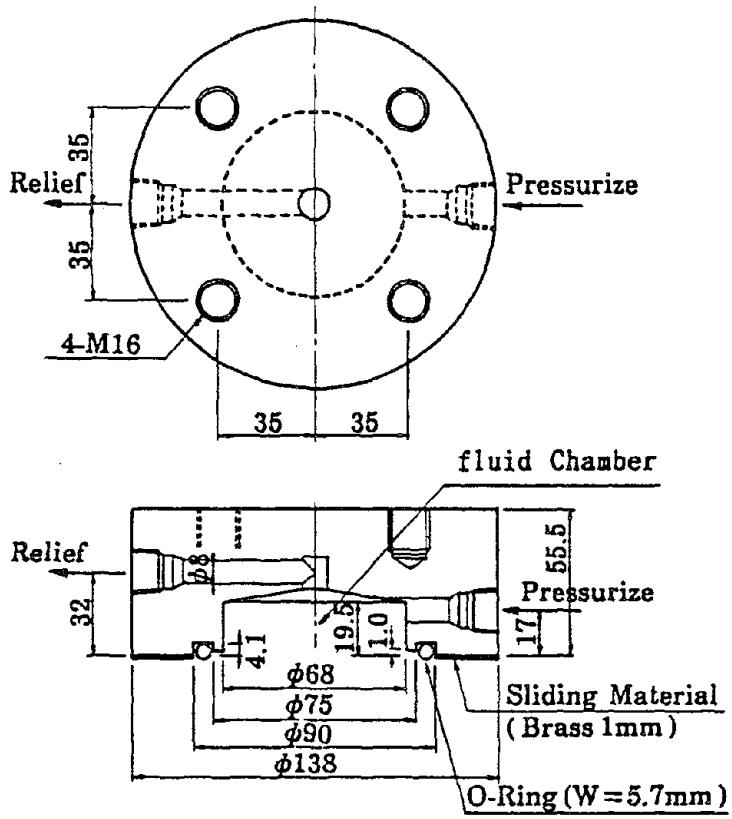

Figure 3.3: Friction Controllable Sliding Bearing

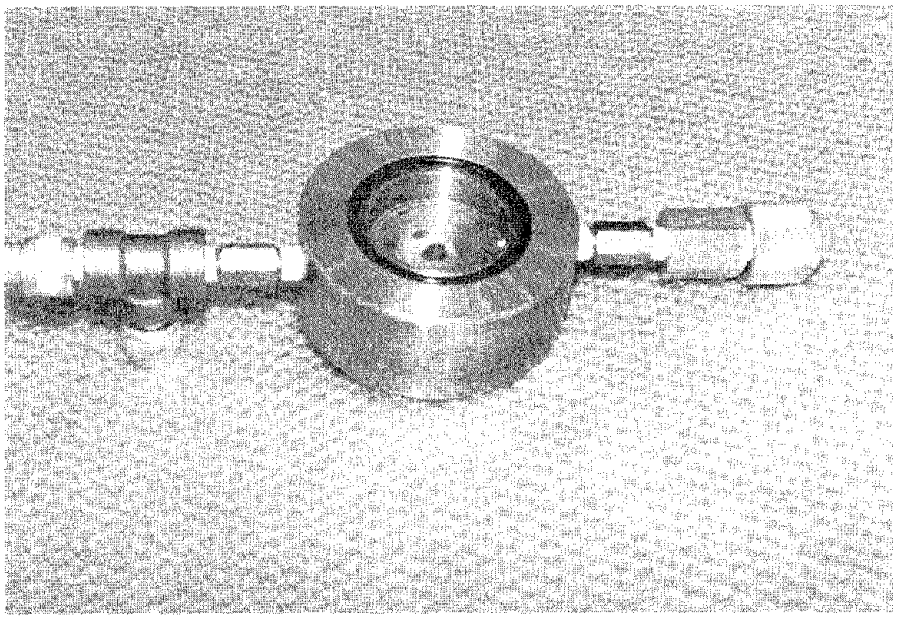

Figure 3.4: Friction Controllable Sliding Bearing for Experiment

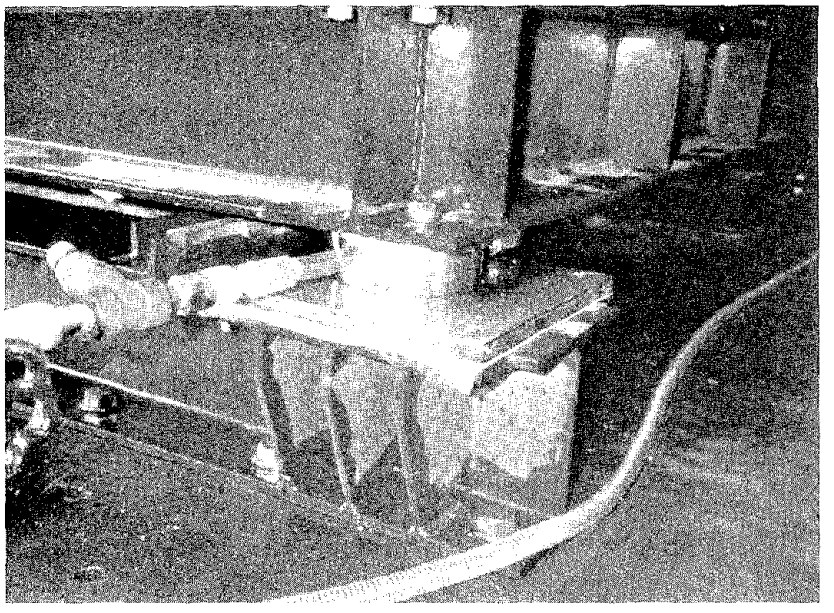

Figure 3.5: Friction Controllable Sliding Bearing in Experiment

3.2 Control System and Instrumentation

A block diagram of the control system is shown in Fig. 3.6 [17, 18]. The controller is a 16 bit micro-computer (80286) with a numerical co-processor (80287) to facilitate faster computation. The response signals for feedback purpose are measured by sensors and sent to the micro-computer through 12 bit A/D converter. Then, the control signal is calculated according to one of the feedback control algorithms described in the previous section, and sent to the servo valve and servo amplifier through a 12 bit D/A converter to control the fluid pressure in the bearing chamber.

A computer code for control implementation in experiments is developed using the C language.

Sensors are placed to monitor (1) accelerations on the shaking table and on the structural model, (2) relative displacement between the shaking table and the model, and (3) fluid pressure at each fluid chamber and at the servo valve. The locations of the sensors are also shown in Fig. 3.1.

The measurement performed by the displacement sensor D4 and the accelerometer on the structural model A4 are used for the feedback control purpose, while the pressure at the servo valve P5 is used for the analog regulation of the pressure in the servo valve.

Figure 3.7 is a photograph showing the computer, some of the measuring and recording equipment used in the experiments.

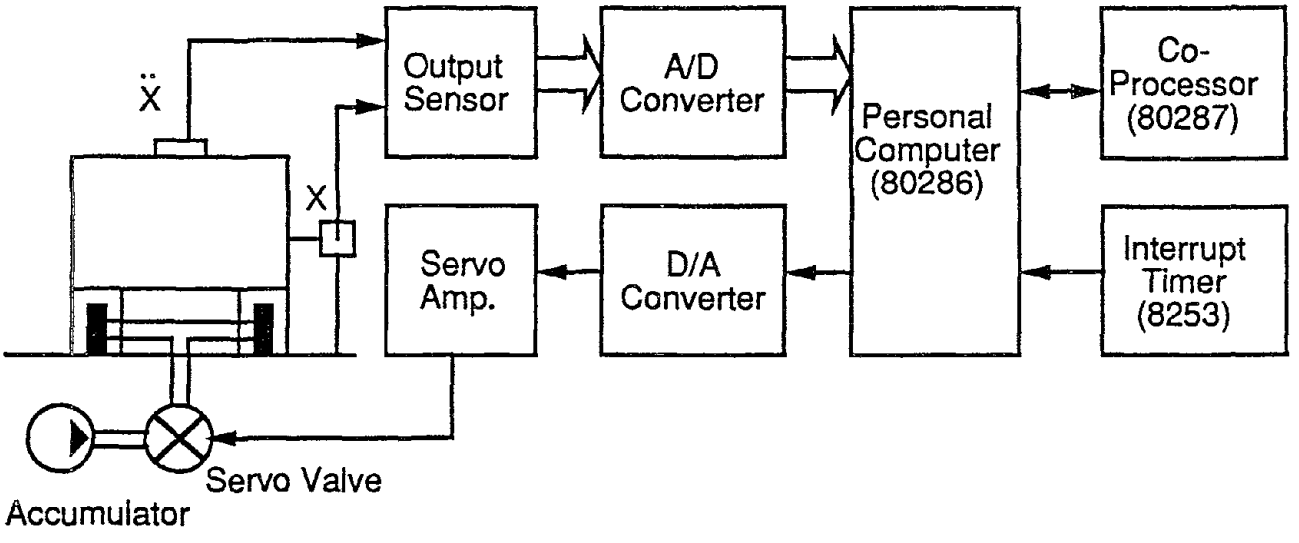

Figure 3.6: Block Diagram of Control System

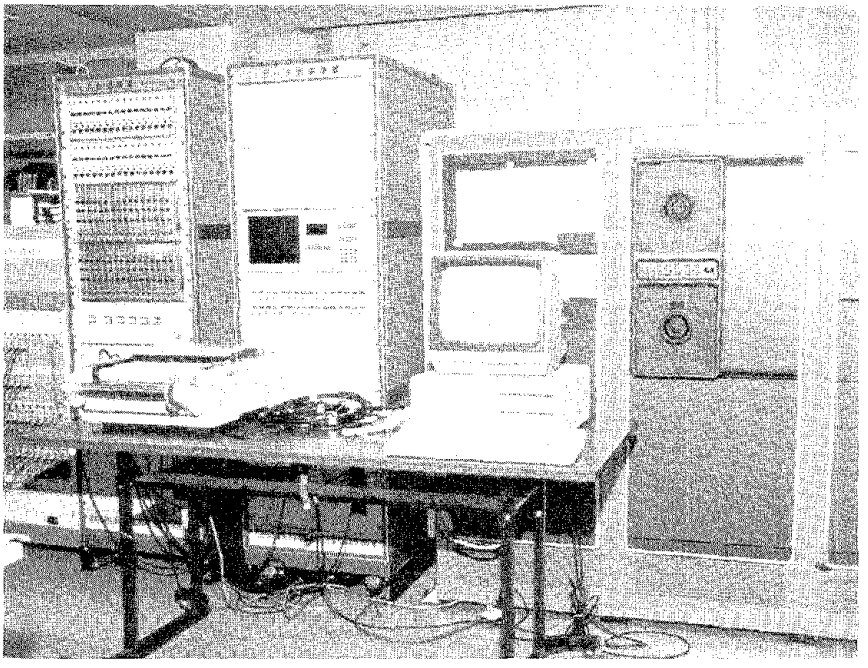

Figure 3.7: Computer and part of control system in experiment

3.3 Experimental Program

The experimental program, as described in Table 3.1, involves the following three isolation types;

1. Passive isolation

   The pressure control signal is kept constant at a certain value for each shaking table experiment (at 10, 20, 30, 40 and 45 kgf/cm^2).

2. Hybrid isolation using bang-bang control

   The pressure control signal is switched between the following two values: u_{max} = 45 kgf/cm^2 and u_{min} = 10 kgf/cm^2.

3. Hybrid isolation using instantaneous optimal control

   3a. algorithm with time delay

   3b. algorithm without time delay

   The pressure control signal is bounded by u_{max} = 45 kgf/cm^2 and u_{min} = 10 kgf/cm^2 for both cases. In case 3a, both response acceleration and sliding displacement are used for the feedback purpose with the feedback gains F_f = 1.0 kgfs^2/cm^3 and F_d = -45.0 kgf/cm^3 in Eq. 2.25. In case 3b only sliding displacement is used, as indicated in Eq. 2.30, with the feedback gains F = 16.5 kgf/cm^2 and F_d = -16.4 kgf/cm^3. In this case, the pressure control signal is nominally equal to the minimum value at the sliding displacement of 2.5 cm. The value of u_{max} = 45.0 kgf/cm^2 is determined by the maximum pressure which can be applied to the bearing chamber, depending on the

Table 3.1: Experimental Series

SERIES	PURPOSE	INPUT MOTION
1. Passive Isolation	1. Isolation performance 2. Identification of friction -pressure relationship	El Centro (NS) 100,200,300,400,450 gal Hachinohe (NS), 300 gal Taft (EW), 300 gal
2. Bang-Bang Control	1. Isolation performance 2. Identification of time delay of control device	El Centro (NS), 300gal Sinusoidal waves, 1 Hz 150 gal and 250 gal
3. Optimal Control without time delay	1. Isolation Performance 2. Study of time intervals 3. Effect of feedback gains 4. Effect of window comparator	El Centro (NS) 100,200,300 gal Hachinohe (NS), 300 gal Taft (EW), 300 gal
4. Optimal Control with time delay	1. Isolation performance 2. Study of window comparator	El Centro (NS) 100,200,300 gal Hachinohe (NS), 300 gal Taft (EW), 300 gal

vertical load identical to the structural weight equally shared by the four bearings:

$$u_{max} = \frac{W}{4S} * \lambda = 45.0 \ kgf/cm^2 \tag{3.1}$$

where, S is the vertically projected area of the fluid chamber of each bearing with the value of 57.7 cm^2 , and λ is a safety coefficient with the value $\lambda = 0.87$ providing some margin of safety. On the other hand, the value of $u_{min} = 10$ kgf/cm^2 is set because the experiment indicates that the pressure response p to the control signal u is too slow for the control to be effective if it is below 10 kgf/cm^2.

The relationship between the pressure and the coefficient of friction is identified from the passive isolation experiments which are refered to as Experimental Series 1. The dynamic response characteristics of pressure and friction to the control signal is identified from the

bang-bang control experiment in Experimental Series 2. The time intervals for measurement and control are examined using the optimal control experiments without time delay (Experimental Series 3), and the appropriate values of the window comparator are studied using the optimal control experiments with and without time delay (Experimental Series 4). More importantly, the results of these experiments are used to examine and compare the isolation performance of each isolation type under different input motions at differing levels of intensity. These experimental series and their purpose are summarized in Table 3.1.

The shaking table experiments were conducted under one-dimensional horizontal motion (as shown in Fig. 3.1). The El Centro (NS, 1940) record was used as ground input motion for most of the experiment cases, by linearly adjusting the maximum acceleration to 100, 200, 300 400 and 450 gal as shown in Table 3.1, where it is also shown that Hachinohe NS, Taft EW , and sinusoidal waves were also used in some experiment cases.

SECTION 4

EXPERIMENTAL RESULTS

4.1 System Identification

4.1.1 Response of Pressure to Control Signal

The response characteristics of pressure to control signal have been identified by the shaking table experiment performed under El Centro 300 gal excitation in Series 2 (bang-bang control). The control signal was switched between 10 kgf/cm^2 and 45 kgf/cm^2. One set of the recorded time histories observed in this experiment are shown in Fig. 4.1.

A first order time delay model is assumed between the control signal and the pressure response as described in Eq. 2.6. The time constant T in the equation has been identified by minimizing the sum of the square errors between the pressure response from the experiment and that from the computer simulation. It is observed that the time delay of the pressure response to the control signal depends on whether the pressure is increased or decreased. Therefore, the time constants T_i under increasing pressure and T_d under decreasing pressure are identified separately as shown in Figs. 4.2 and 4.3. Figure 4.2 plots the sum of the square

error defined as $\sum_k (p_{sim}(t_k;T_i) - p_{exp}(t_k))^2$ where $p_{exp}(t_k)$ = pressure value observed in the experiment at $t = t_k$, and $p_{sim}(t_k;T_i)$ = simulated value at $t = t_k$ with T_i being used as time constant. The summation is over those time intervels in the entire time history where the pressure increases. Figure 4.3 plots the sum of the square errors for the time intervals where pressure decrease. The curves in these two figures indicate reasonably well defined optimal values for T_i and T_d, with $T_i = 0.029$ sec and $T_d = 0.035$ sec.

Figure 4.4 shows, in solid line, part of the time history of pressure response from the bang-bang control experiment. Also the pressure response obtained by computer simulation is shown in Fig. 4.4, in dashed line, using the first order time delay model of Eq. 2.6 with the optimal values of the time constants identified above. The simulation result is in good agreement with the experimental result, implying that the analytical model for the relationship between pressure response and control signal, Eq. 2.6, with the identified value of time constants represents the reality very well.

4.1.2 Relationship Between Friction and Pressure

In the structural model considered, the absolute value of response acceleration equals the normalized friction force f ($f = \mu\ g$) when the model is sliding as indicated in Eq. 2.2. Therefore, the response acceleration detected from the sensor can be used to study the behavior of the friction. From the response acceleration observed in Experimental Series 1 (passive isolation) conducted at various levels of constant pressure under El Centro excitation, the relationship between pressure p and normalized friction force f is identified.

As shown in Fig. 4.5, the relationship between the pressure and the normalized friction force follows a linear relationship. The coefficient of friction μ of about 10.2% at the pressure

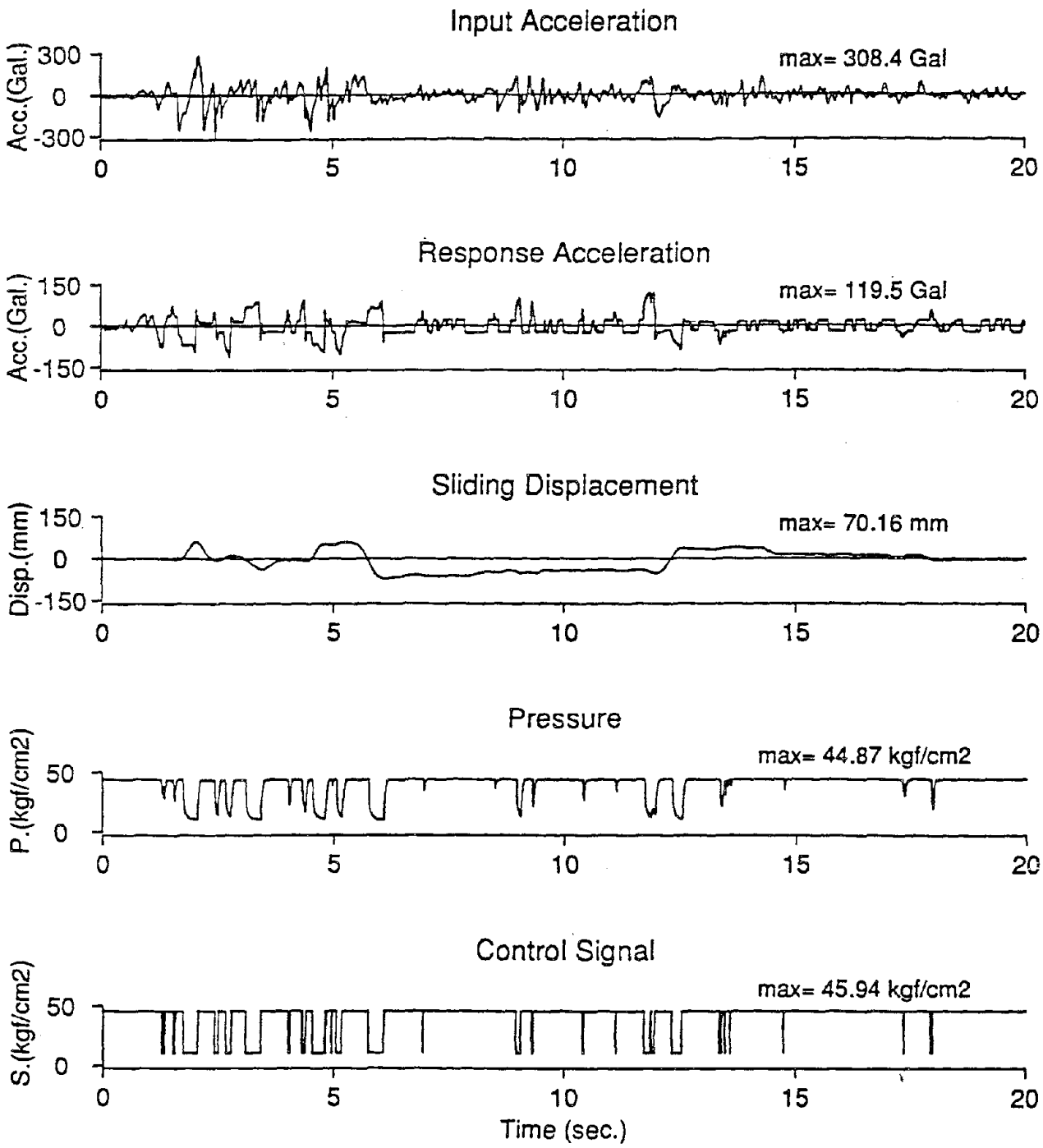

Figure 4.1: Bang-bang Control (Experiment)

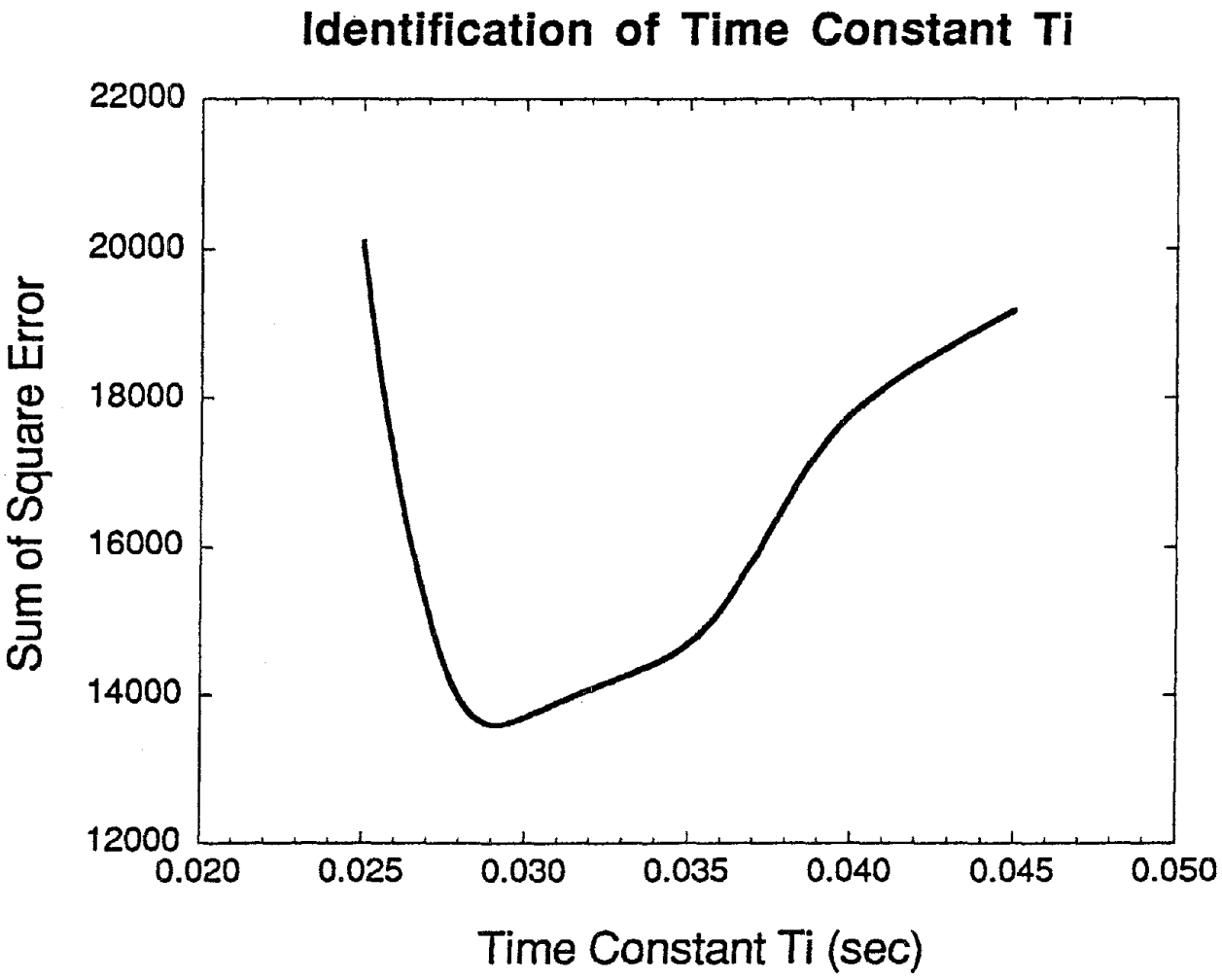

Figure 4.2: Identification of Time Constant T_i

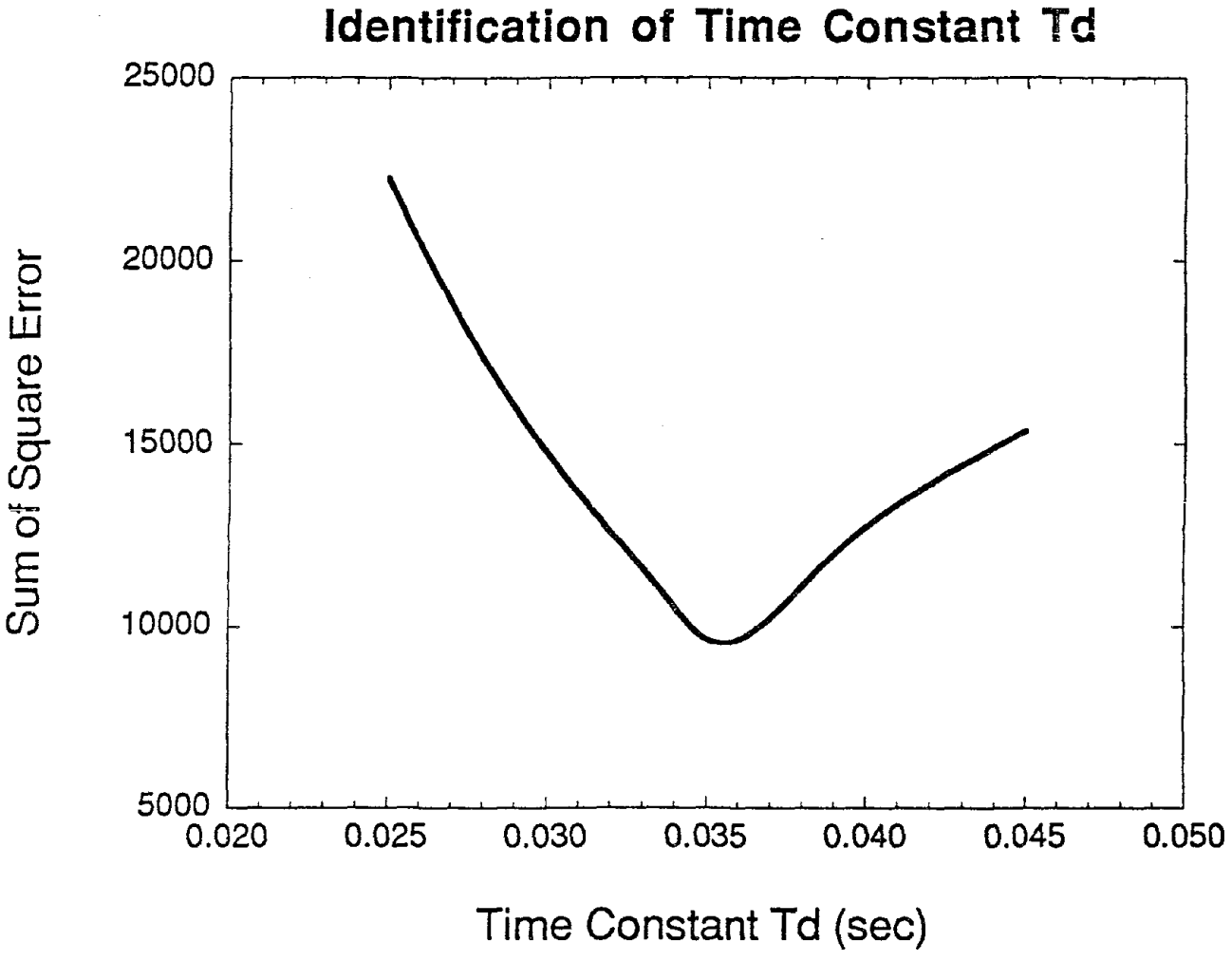

Figure 4.3: Identification of Time Constant T_d

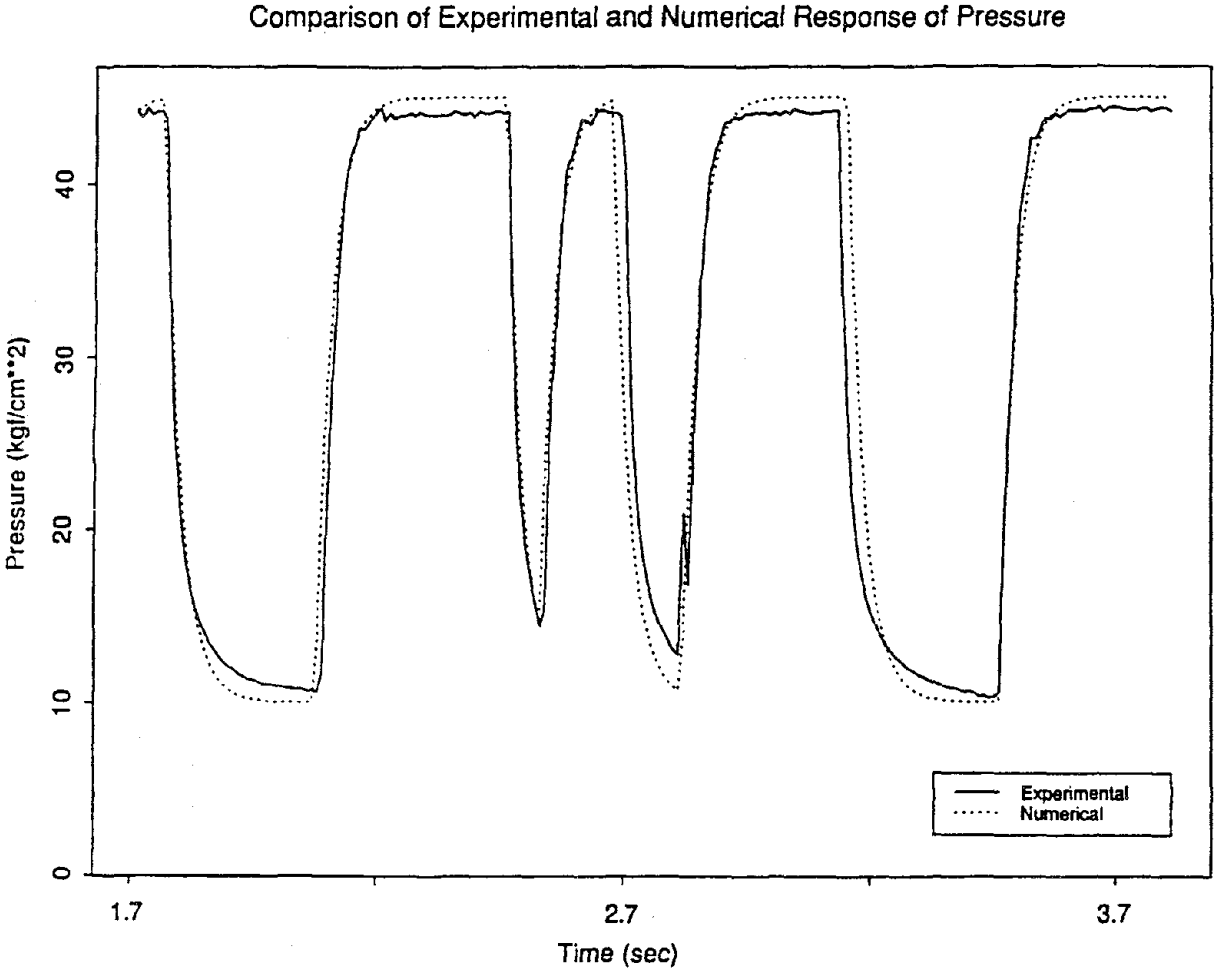

Figure 4.4: Example of Experimental and Simulated Time Histories of Pressure

of 10 kgf/cm^2 can, for example, be reduced to 1.6% at the pressure of 45 kgf/cm^2. Equation 2.7 thus can be used to describe the relationship, and the values of c_1 and c_2 are identified as $c_1 = 2.4\text{cm}^3/\text{s}^2\text{kgf}$ and $c_2 = 124.0\text{cm/s}$. As will be shown in the next subsection, however, the friction force depends not only on the pressure but also on the sliding velocity. In this respect, the value of normalized friction force used in Eq. 2.7 is valid only when the sliding velocity is zero, and therefore it is rewitten as

$$f_0 = -c_1 p + c_2 \tag{4.1}$$

where f_0 is the normalized friction force at sliding velocity of zero.

4.1.3 Dependence of Friction on Sliding Velocity

It is observed from the response acceleration measured in Experimental Series 1 (passive isolation) that the the normalized friction force f decreases with the increase of sliding velocity. In fact, these measurements are used to identify the dependence of friction on sliding velocity.

Figure 4.6 shows an example set of time histories of a passive isolation experiment, in which the pressure was kept at 30 kgf/cm^2, corresponding to the coefficient of friction 5.6%, and the input ground motion was El Centro record with peak acceleration of about 300 gal. From the behavior of the response acceleration, it is assumed that the relationship between the normalized friction force and sliding velocity takes the following analytical form:

$$f = f_0 \frac{k^2}{\dot{x}^2 + k^2} \tag{4.2}$$

where f_0 is the normalized friction at sliding velocity of zero as defined by Eq. 3.2, while k is a constant.

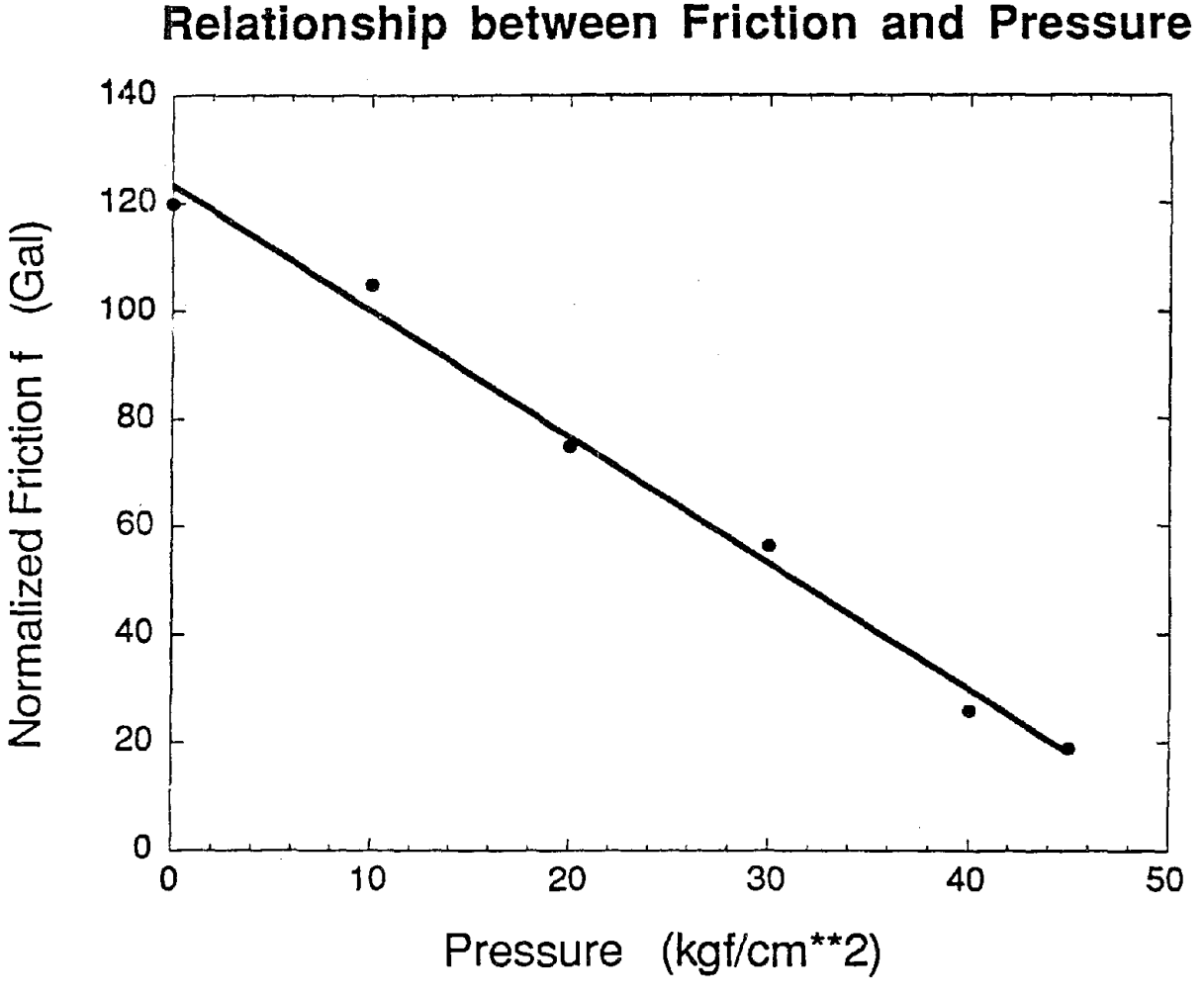

Figure 4.5: Relationship between Pressure and Normalized Friction Force

Table 4.1: Identified Parameters

T_i	29 ms	c_1	2.4 $cm^3/(s^2kgf)$
T_d	35 ms	c_2	124.1 cm/s^2
k^2	0.11 cm/s		

The value of k^2 is identified by minimizing the sum of the square errors between response acceleration shown in Fig. 4.7 and that from the numerical simulation over the entire time history ($\sum_k ((\ddot{x}+\ddot{z})_{sim}(t_k;k) - (\ddot{x}+\ddot{z})_{exp}(t_k))^2$). As shown in Fig. 4.7, the optimal value of k^2 is 0.11 m^2/s^2, at which the sum of square error is minimum.

It is found that $k^2 = 0.11$ m^2/s^2 is also the optimal value for other passive isolation experiments where the pressure is kept at 10, 20, 40 and 45 kgf/cm^2. Figure 4.8 shows part of the experimental and simulated time histories of response acceleration for the passive isolation performed under $p = 30$ kgf/cm^2. Again, the simulation result matches the experimental result very well, implying that the identified model for friction closely represents the reality.

4.1.4 Response of Friction to Control Signal

Summarizing the identification results, the response of friction force to control signal can be modeled by the following equations:

$$T\dot{p} + p = u \tag{4.3}$$

$$f_0 = -c_1 p + c_2 \tag{4.4}$$

$$f = f_0 \frac{\dot{x}^2}{\dot{x}^2 + k^2} \tag{4.5}$$

The values of parameters T, c_1, c_2, k^2 identified are summerized in Table 4.1.

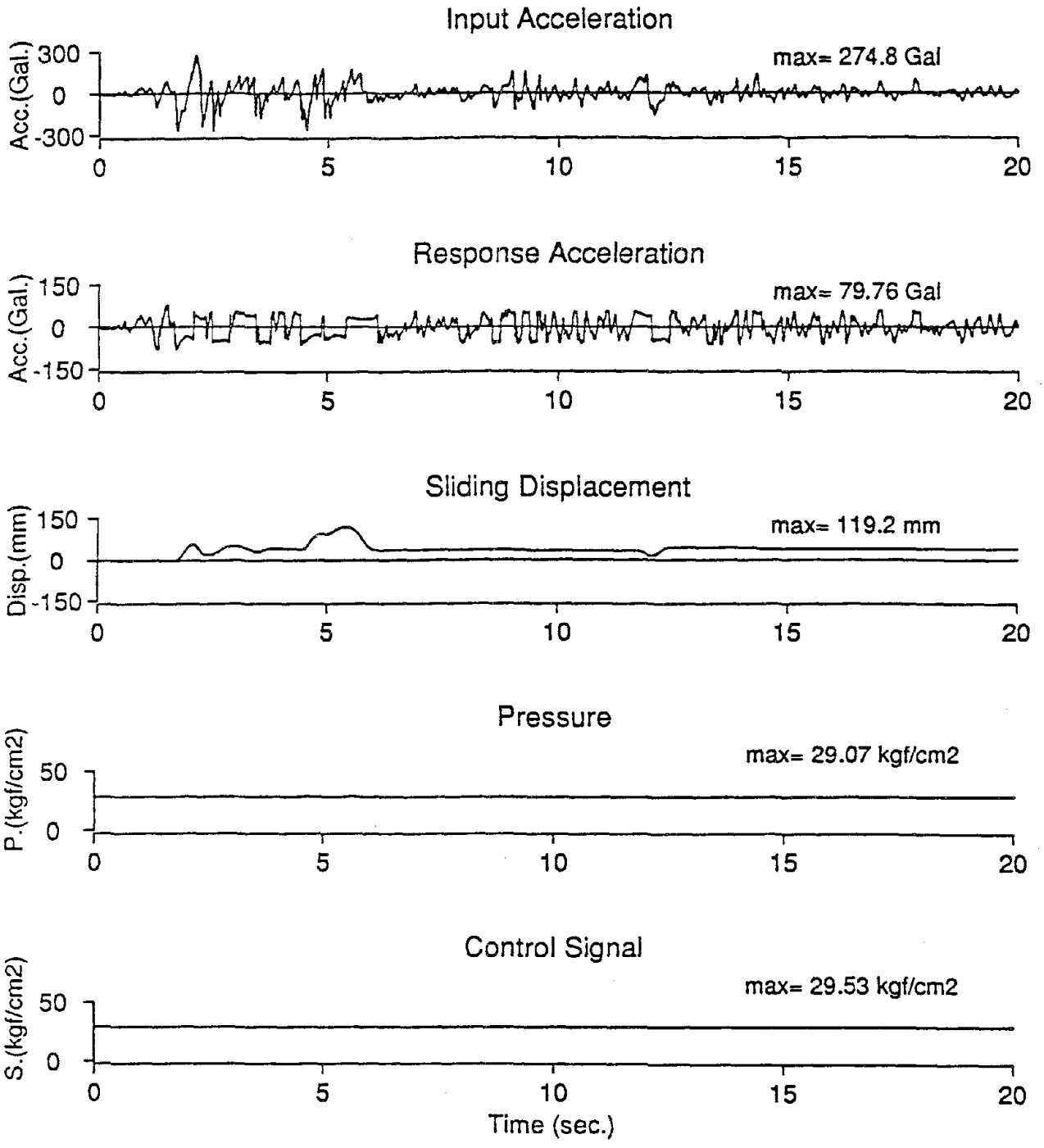

Figure 4.6: Passive (Experiment)

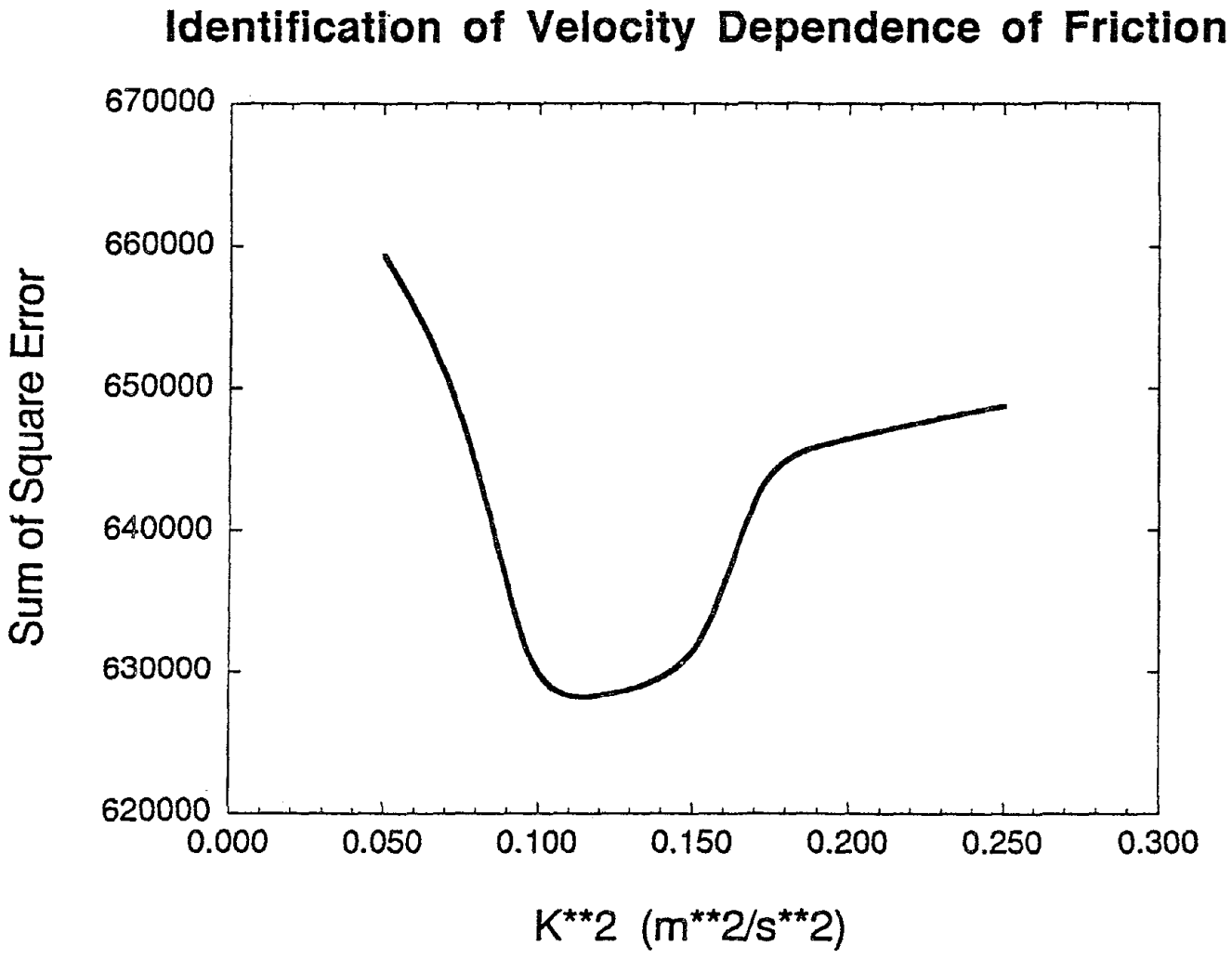

Figure 4.7: Identification of Constant k^2

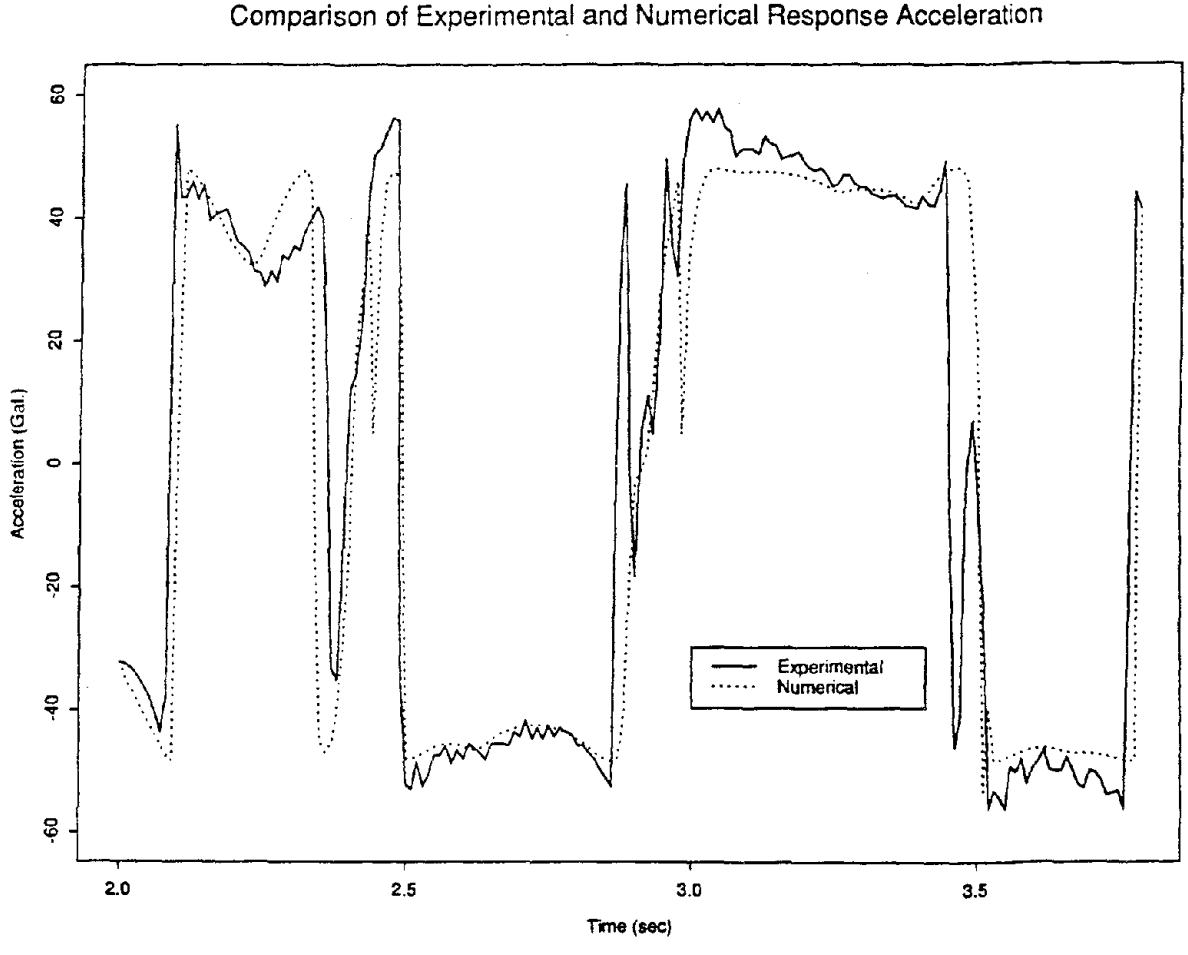

Figure 4.8: Example of Experimental and Simulated Time Histories of Acceleration

4.2 Passive and Hybrid Isolation

Typical experimental results from four series of experiments utilizing the techniques of passive isolation, bang-bang control, and instantaneous optimal control with and without time delay are compared with each other. These results are obtained under the El Centro (NS, 1940) ground motion with the peak acceleration of about 300 Gal. Figures 4.6 and 4.1 shown before give two sets of time histories for response acceleration, sliding displacement, pressure, and pressure control signal corresponding to Experimental Series 1 and 2 respectively, while Figs. 4.9 and 4.10 show two sets corresponding to Experimental Series 3 and 4.

In the passive isolation results as shown in Fig. 4.6, the pressure in the bearing chamber was kept at 30 kgf/cm^2, corresponding to the coefficient of friction 5.6%. A large residual sliding displacement of 62 mm after the earthquake is observed.

In the bang-bang control experiment shown in Fig. 4.1, the pressure control signal is switched between 10 kgf/cm^2 and 45 kgf/cm^2. The maximum and minimum response accelerations are consistent with the accelerations of the passive isolation cases of p = 10 kgf/cm^2 and 45 kgf/cm^2 respectively. However, the residual displacement is almost zero and the maximum sliding displacement is about 20 % less than the passive isolation, showing the effectiveness of the bang-bang control in reducing the sliding displacement.

Figures 4.9 and 4.10 respectively show the results of hybrid isolation experiments using instantaneous optimal control without and with time delay, in which the feedback gains are set to: F_f = 1.0 kgfs^2/cm^3 and F_d = -45 kgf/cm^3, and F_f = 16.5 kgf/cm^2 and F_d = -16.4 kgf/cm^3 with time delay. In both cases, the pressure control signal is confined between u_{max} = 45 kgf/cm^2 and u_{min} = 10 kgf/cm^2. The response of instantaneous optimal control,

depicted in Figs. 4.9 and 4.10, show the results similar to that of the bang-bang control experiment. This is because the feedback gains used in these experiments force the control signal to reach the minimum value of 10kgf/cm^2 primarily for the purpose of confining the sliding displacement to a small value under the ground acceleration as large as El Centro earthquake with peak acceleration of about 300 gal. The instantaneous optimal control with time delay (Fig. 15(a)) shows the best control performance among the three control algorithms developed and tested in the experiments.

The difficulty of starting initial slide associated with the passive system is alleviated in the hybrid systems.

The experimental results of passive and hybrid isolation under the Hachinohe (NS) and Taft (EW) are shown in the Appendex A.

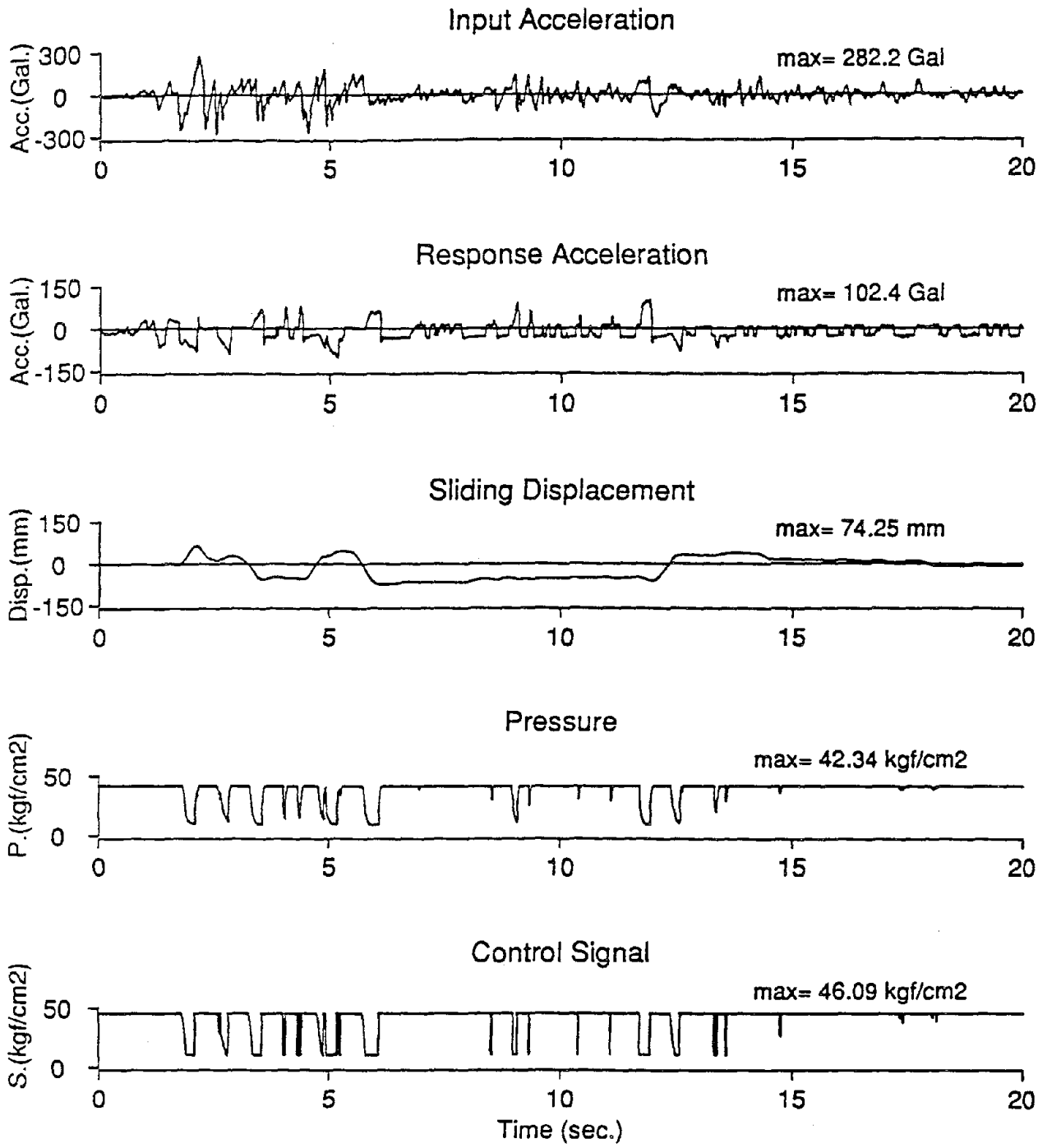

Figure 4.9: Instantaneous Optimal Control without Time Delay (Experiment)

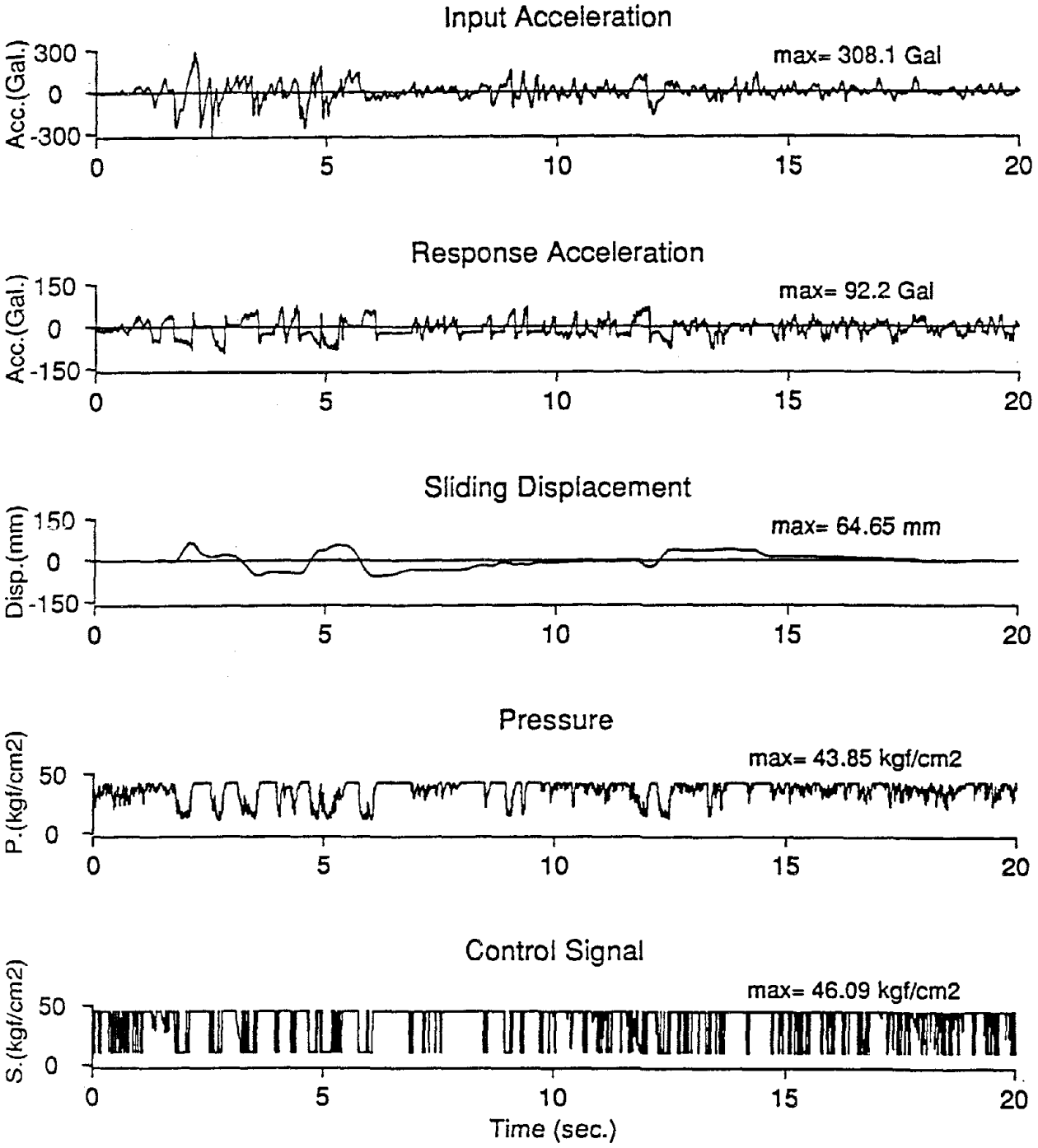

Figure 4.10: Instantaneous Optimal Control with Time Delay (Experiment)

4.3 Comparison of Hybrid and Passive Isolation

The performance of the hybrid isolation system is compared to that of the passive isolation system. Figures. 4.11 and 4.12 show the maximum response acceleration, maximum sliding displacement, and the residual displacement of the structural model with passive or hybrid isolation system under El Centro records of different peak ground acceleration. Hybrid isolation results shown in these figures are those under instantaneous optimal control algorithm without time delay.

In the passive isolation, if a small friction coefficient, for example 1.6%, is used, a high level of isolation performance is expected since the response acceleration is reduced to a small level. In this case, however, the maximum displacement becomes excessive very rapidly as the input earthquake becomes more intense. On the other hand, if a large friction coefficient such as 10.2% is used, the sliding displacement can be confined within a relatively small range. However, the isolation performance in this case is limited in the sense that the acceleration can not be satisfactorily reduced. Particularly for small to medium earthquakes with peak acceleration less than 100 gal, this passive sliding isolation system does not function at all, thus the response acceleration equals the input acceleration. Such acceleration might damage the sensitive equipment inside the building.

The hybrid isolation system, however, can alleviate these problems associated with the passive isolation system. For small to medium earthquakes, the friction can be controlled to a very small level to make the structure slide easily, so that the response acceleration can be considerably reduced. For large earthquakes, the friction is controlled to prevent the excessive sliding displacement, while the response acceleration can also be kept at a small level. Another advantage of the hybrid system is clearly seen in Fig. 4.12 where the residual

sliding displacement can be maintained almost at zero level.

Experimental results verify that the proposed friction controllable sliding system does make the conventional passive sliding isolation system effective for all intensitics of earthquake.

Comparison of Response Acceleration

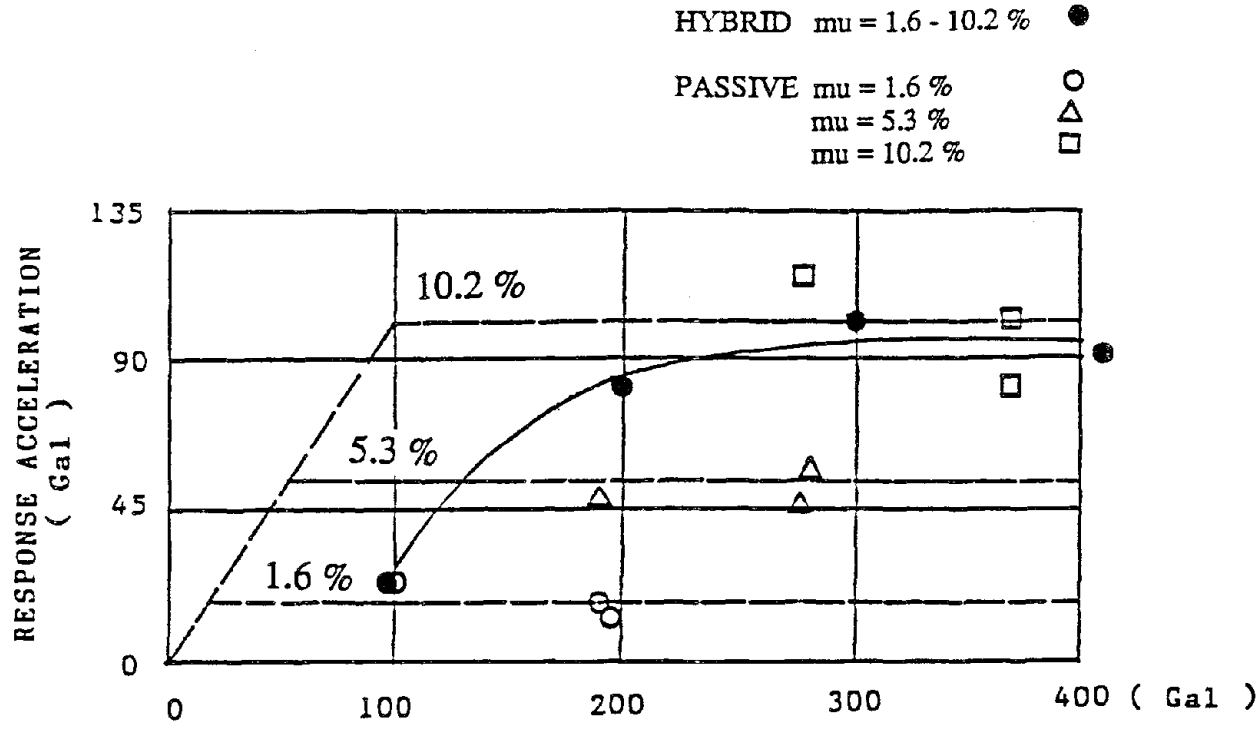

Comparison of Sliding Displacement

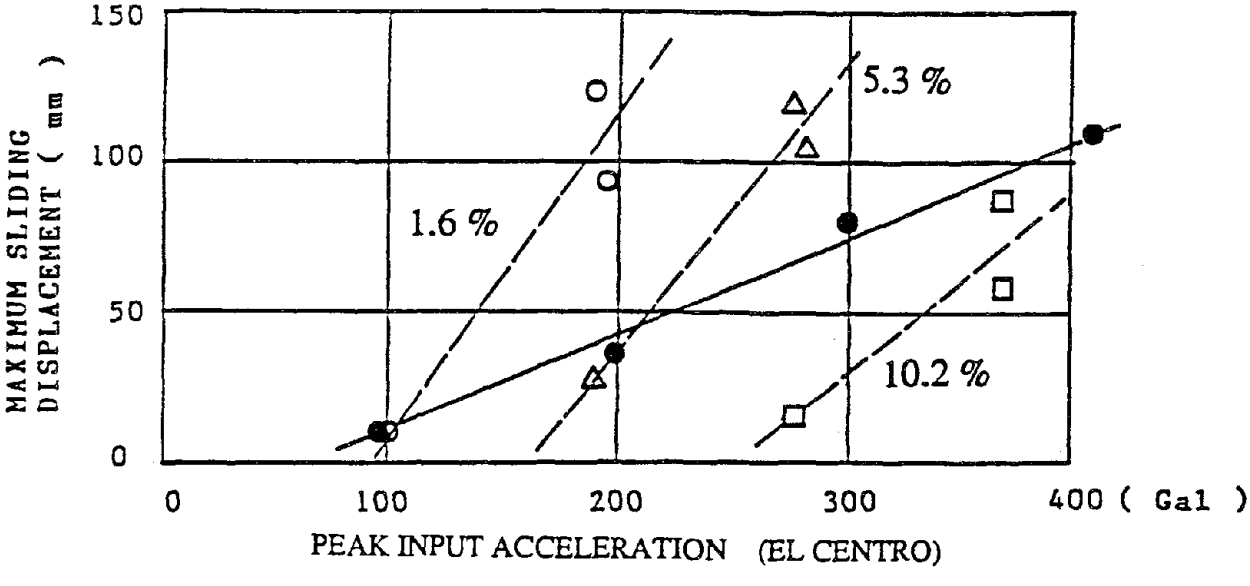

Figure 4.11: Comparison of Passive and Hybrid Isolation

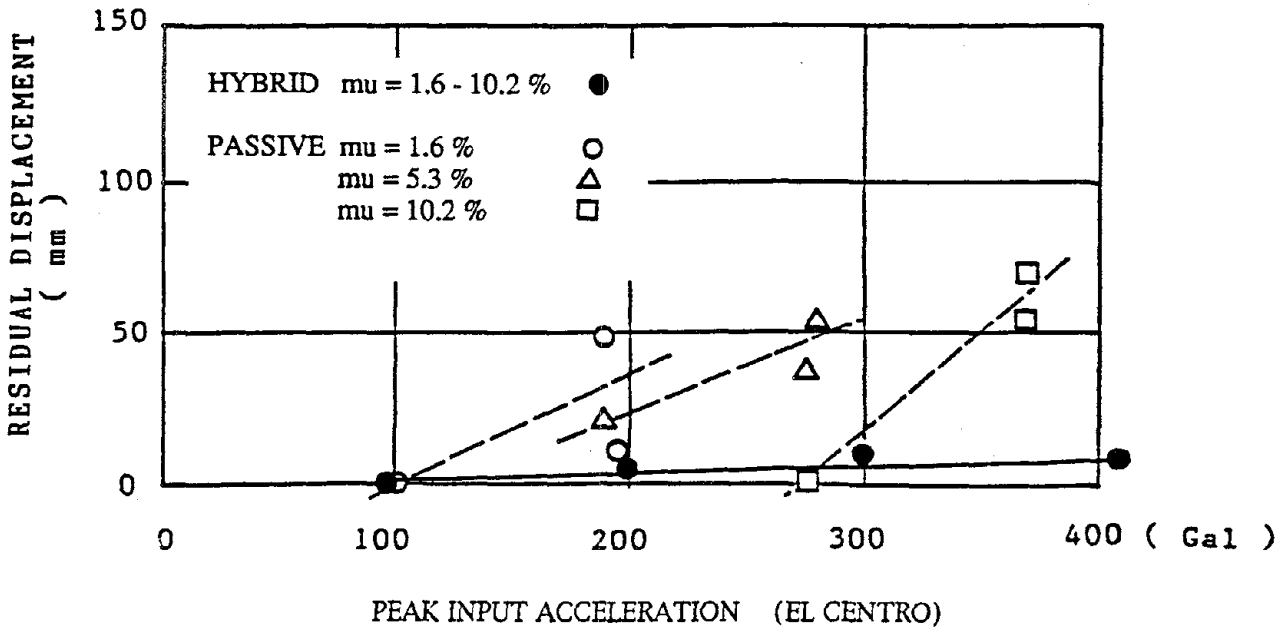

Figure 4.12: Comparison of Passive and Hybrid Isolation (Residual Displacement)

4.4 Study of Control Parameters

The effects of control parameters, such as the time interval of control Δt_c and the threshold value for the window comparator, on control performance have been studied in shaking table experiments. On the basis of these studies, the appropriate values of these parameters are determined. Although the values of feedback gains were also examined in a few cases of shaking table experiments, they were determined by computer simulation analysis.

4.4.1 Time Interval of Control

The continuous-time control algorithms developed in Section 2 can only be executed in the discrete time since a digital computer is used for on-line computation and control execution. As a consequence, response measurements are digitized as feedback signals, while control signal is sent in the form of piecewise step functions through the analog-digital converter as shown in Fig. 3.6. Hence, they are not continuous functions as called for by continuous-time control algorithms, and usually the larger the time interval for control execution, the worse the control performance becomes.

For this reason, the effect of the time interval of control on control performance has been studied in shaking table experiments performed for hybrid isolation system. The response time histories obtained in the experimental case identified as 6-3 with the time interval of control $\Delta t_c = 0.030$ sec, and experimental case identified as 6-6 with $\Delta t_c = 0.004$ sec, are shown respectively in Figs. 4.13 and 4.14. Both cases are under instantaneous optimal control without consideration of time delay, and are subjected to El Centro 300 Gal input earthquake. The time interval for the measurement of feedback signals are $\Delta t_d = 0.002$ sec in both cases.

In the response acceleration shown in Fig. 4.13 (Case 6-3), impulsive response behaviors are observed (denoted by ∇). They are, however, mostly eliminated in Case 6-6 as shown in the same figure indicating the improvement of control performance by reducing the time interval of control. The sliding displacements, however, show little difference between these two cases as seen in Fig. 4.14.

Further inverstigation shows that the time interval of control smaller than 0.004 sec does not significantly improve control performance. Hence, the time interval of control Δt_c has been set at 0.004 sec in all other control experiments.

It is also interesting to find that the time interval does not change the basic behavior of the structual response without introducing instability. For example, even the time interval as large as 0.03 sec does not introduce the instability of the control system as shown in Figs. 4.13 and 4.14. In this sense, this hybrid control system is quite robust.

4.4.2 Window Comparator

From the control experiments, it was found that there was some high frequency noise in the measurement of feedback signals which resulted in undesirable control signal. In fact, the use of the feedback signal including such high frequency components in experiments produced highly inefficient control results. To alleviate this difficulty, a practical method called "window comparator" is used. The method simply defines a certain threshold value, for the increment of a feedback signal over a certain time interval. If the increment is below the threshold, the variation in the feedback signal is considered as noise and the feedback signal is considered unchanged over that time interval.

The appropriate threshold values for displacement and acceleration signals were studied

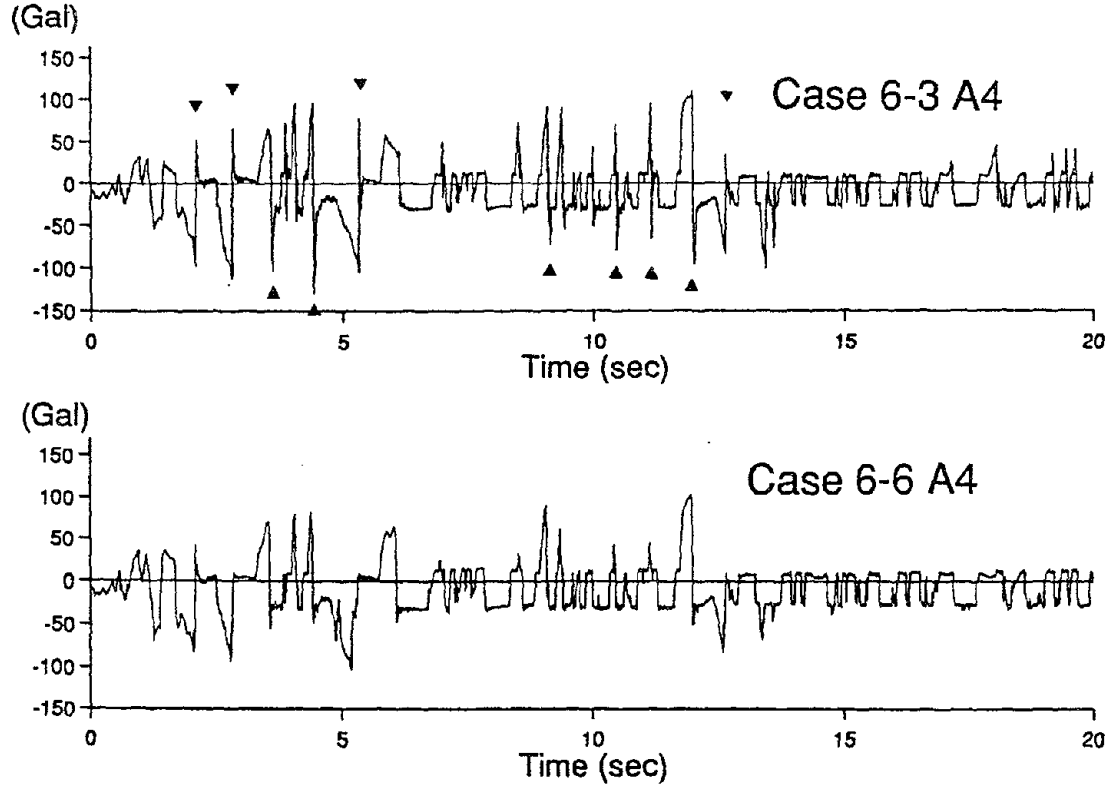

Figure 4.13: Effect of Control Time Interval on Response Acceleration

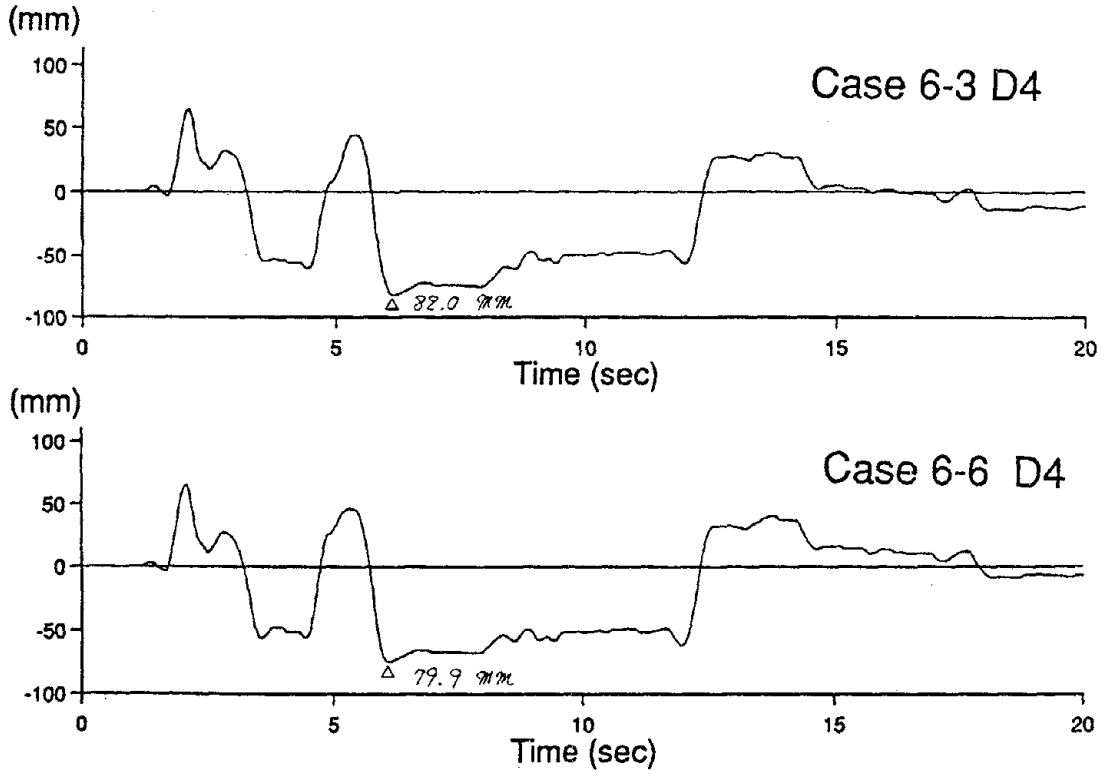

Figure 4.14: Effect of Control Time Interval on Sliding Displacement

respectively in hybrid isolation experiments using instantaneous optimal control with and without time delay. As a result, the threshold value for displacement signal was determined to be $\Delta x = 0.02$ cm for every two control time intervals of 0.008 sec, and the threshold value for acceleration signal was determined to be $\Delta(\ddot{x} + \ddot{z}) = 0.75$ gal for each control time interval of 0.004 sec. The control results are dramatically improved when these threshold values are used. To examine the significance of the threshold values, the increment Δx measured in displacement x measured for every time interval of 0.008 sec from an optimal control experiment is plotted at the end of each time interval as shown in Fig. 4.15, together with time history of displacement. This figure shows that the threshold value equal to 0.02 cm for the displacement increment consistently removes the noise-like high frequency components of the feedback signal.

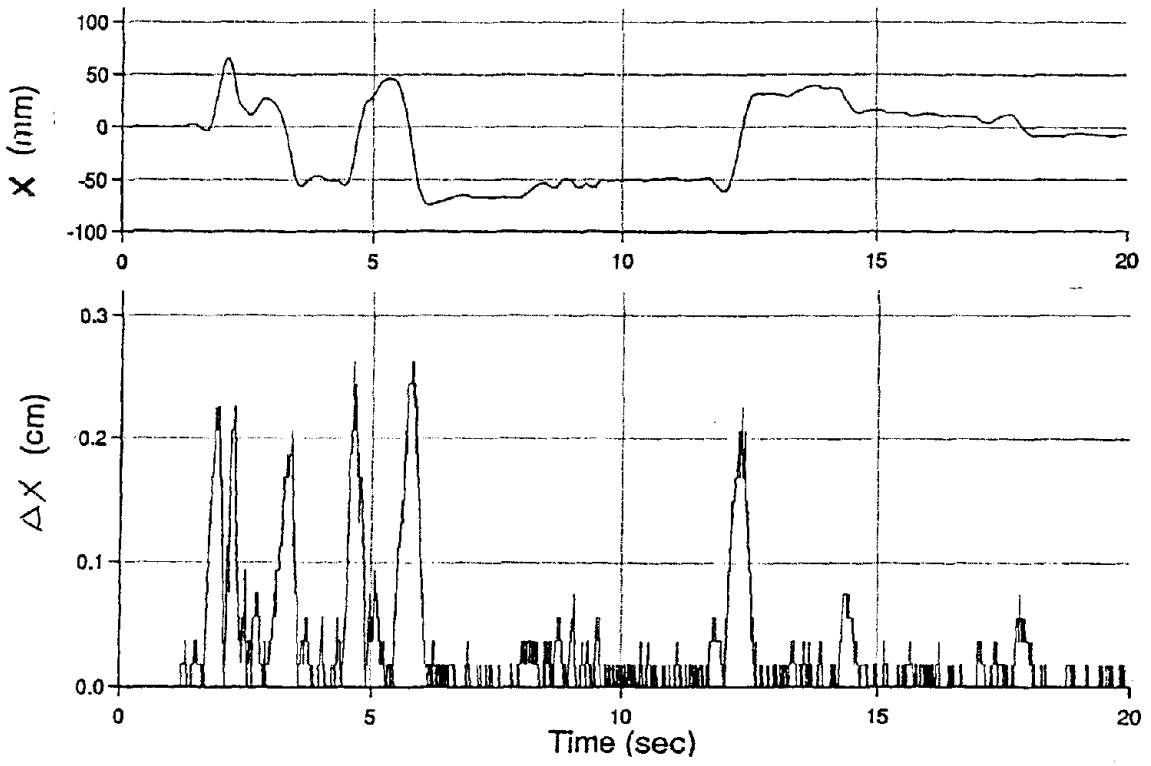

Figure 4.15: Study of Window Comparator

SECTION 5

NUMERICAL SIMULATION

A computer program for the simulation of seismic response of the structure under the hybrid or passive isolation system has been developed. Analytical models presented in the preceding sections, which are based on careful identification experiments, are utilized for computer simulation of experimental results. In this section, it will be demonstrated that these analytical models describe the real system accurately, by carefully comparing the numerical simulation results based on these models with the experimental results.

5.1 Analytical Model and Techniques for Numerical Simulation

The equations of motion of the structural model shown in Eqs. 2.1 - 2.5 and the relationships between the pressure control signal and friction described by Eqs. 4.3 - 4.5 are used for computer simulation. The parameters in these equations use the values given in Table 4.1 as identified by experiments.

Based on the Newmark's β scheme, a double precision FORTRAN routine for numerical integration of the equations of motion and equations of control system has been developed, in which β is selected to 1/6. For the friction system such as under consideration, the precise evaluation are crucial to the accuracy of response calculation when the motion of the structure undergoes transition between the sticking and sliding phases and when the sliding velocity reverses its direction. A time step of Δt is used in the continuous phases of motion, while a much smaller time step Δt is used whenever the phase transits or the velocity reverses its direction. The following computational algorithm is proposed [19] and used.

In Phase II (sliding phase),

1. If the relative velocity of the model changes its direction, go one time interval Δt back, change the time step from Δt to Δt_t and continue the computation again.

2. When the relative velocity changes its direction again, go one time interval Δt_t back, examine whether or not the structural model goes into sticking phase, according to the criterion for transition given in Eq. 2.5.

3. If it goes into sticking phase, change equation of motion to Eq. 2.1, and alter the time step from Δt_t to Δt.

4. If it continues to slide, reverse the direction of friction force, and continue the computation in sliding phase using the time step Δt.

In Phase I (sticking phase),

1. Examine if the model goes into sliding phase according to the criterion given in Eq.

2.3. If it does, change the equation of motion to Eq. 2.2, and change the time step from Δt to Δt_t for the next time interval Δt.

The accuracy of the simulation results is verified by comparing the results with those by finer time steps Δt_t on several simulation cases, and the time step Δt_t has been determined to be 0.00001 sec . The value of time step Δt should be at least 0.002 sec in the simulation of hybrid isolation, because this value was used as the time interval for the measurement of feedback signals in the hybrid control experiments as mentioned before. In the simulation of the response of the building which is passively isolated, however, the value of the time step $\Delta t = 0.01$ sec is used and it appears to be fine enough for the numerical integration.

5.2 Comparison of Simulation with Experimental Results

Shaking table experimental results described in the preceding sections are simulated by numerical analysis. Some examples of time histories from simulation of passive isolation and hybrid isolation using bang-bang control as well as instantaneous optimal control without and with time delay are shown in Figs. 5.1 - 5.4 respectively, together with the corresponding experimental results. In this respect, several remarks seem in order:

1. On the whole, numerical simulation results show remarkably high degree of agreement with experimental results. This demonstrates that the analytical model with the parameter values used represents the reality very well.

2. In simulation, the static coefficient of friction is assumed to be the same as the sliding coefficient of friction. Therefore, simulation could not show the maximum response acceleration, which is due to the static friction, in the passive isolation experiment.

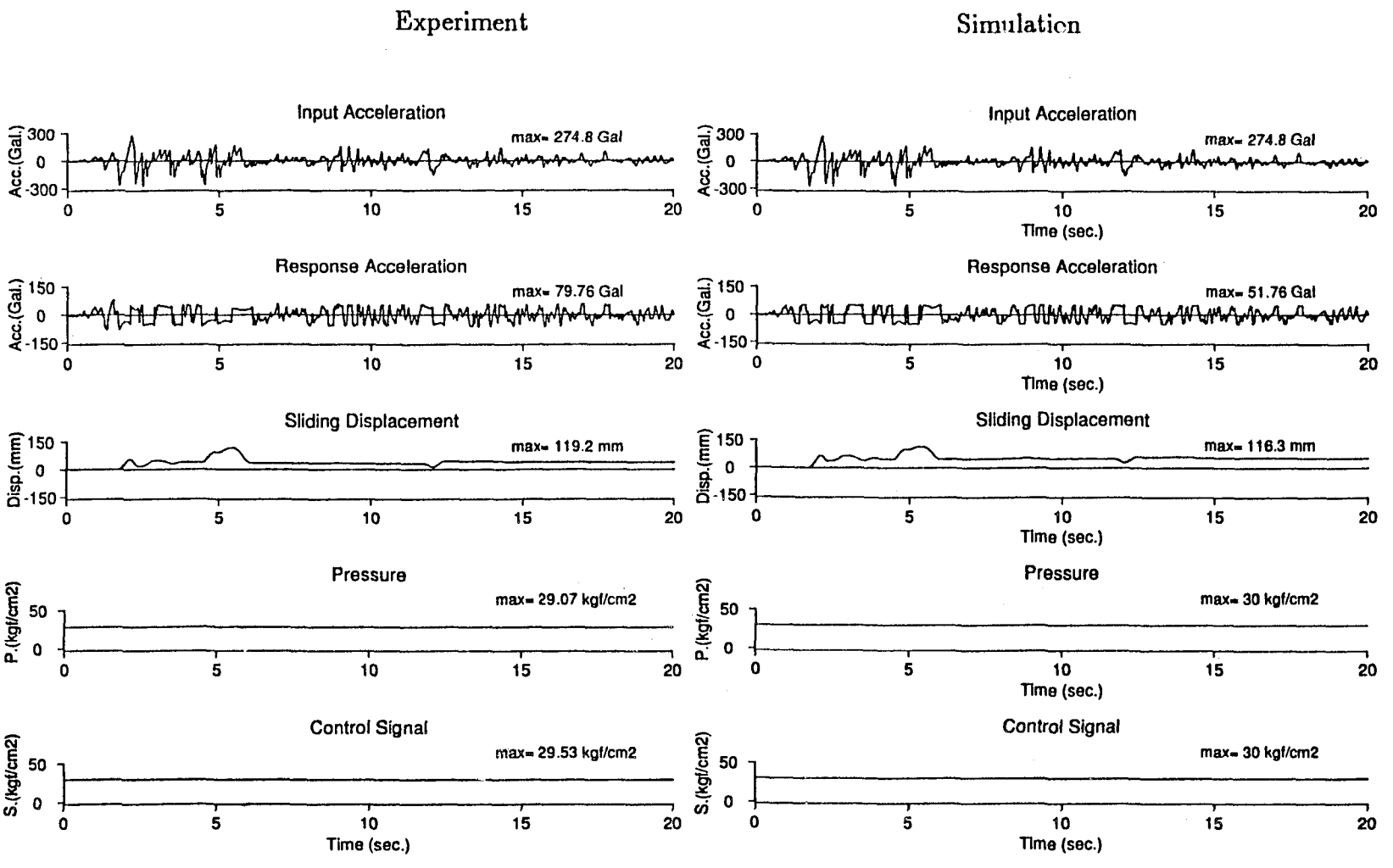

Figure 5.1: Passive Isolation

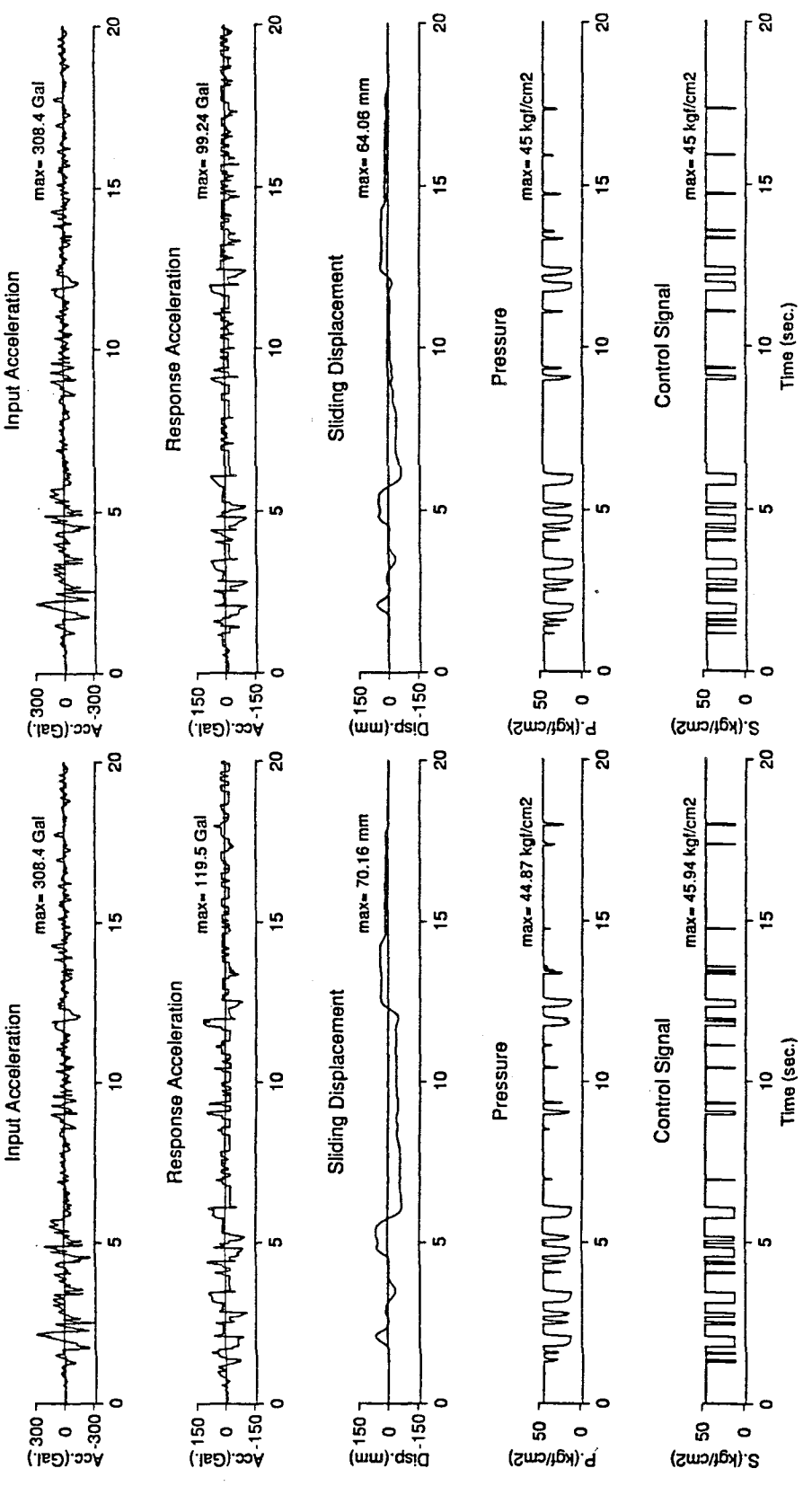

Figure 5.2: Hybrid Isolation under Bang-Bang Control

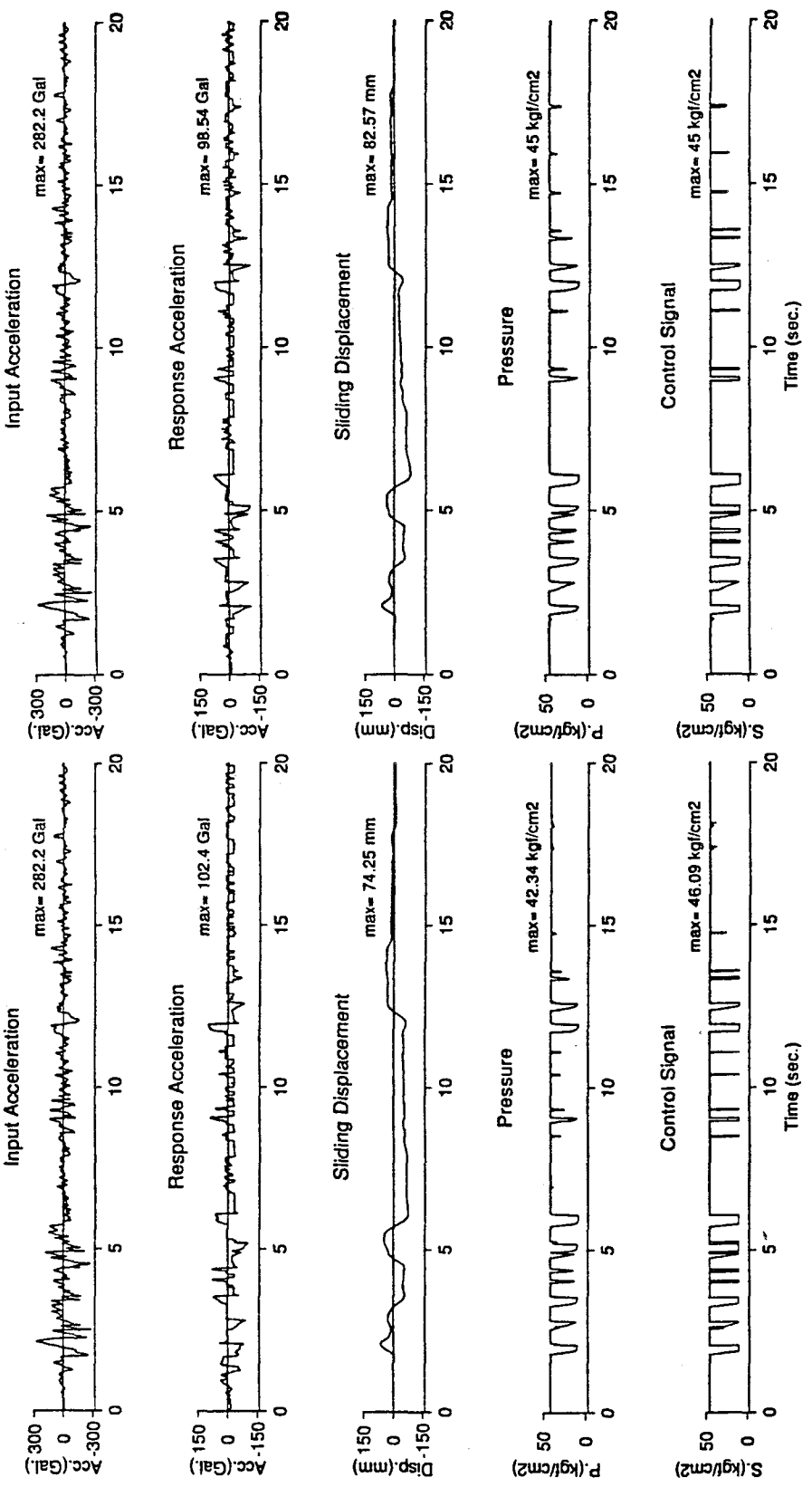

Figure 5.3: Hybrid Isolation under Optimal Control without Time Delay

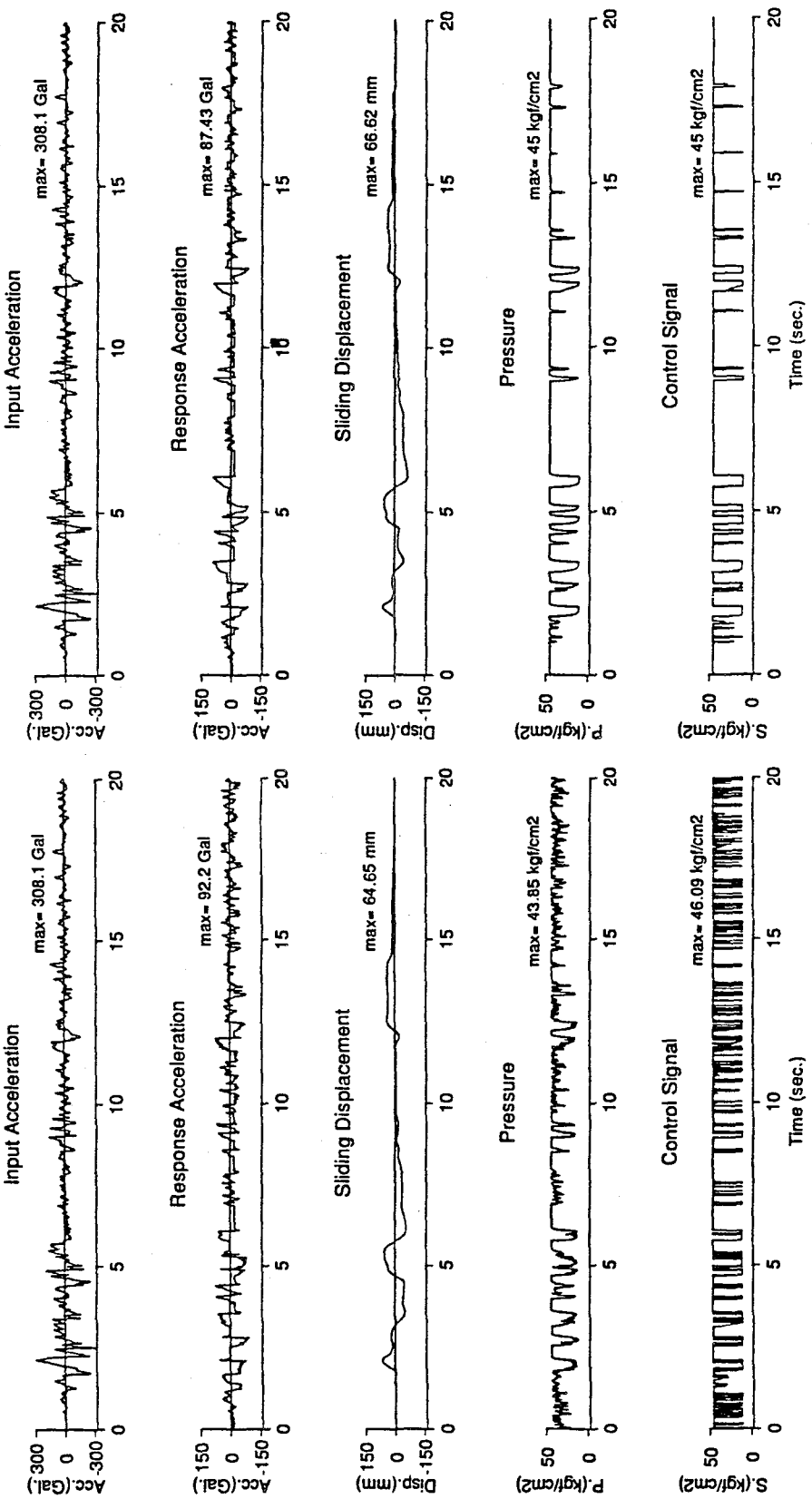

Figure 5.4: Hybrid Isolation under Optimal Control with Time delay

5.3 Robustness of System

In the experiments and computer simulation, it is found that the proposed hybrid isolation system is quite robust.

1. The instantaneous optimal control algorithms in Section 2 are developed on the reduced-order models, ignoring the following aspects in the real models: (i) sticking phase of motion (Eq. 2.1), (ii) influence of sliding velocity on the friction force (Eq. 3.3), and (iii) time delay in the pressure response to the control signal (Eq. 2.6), obviously when developing the algorithm without time delay. However, the reduced-order model did not adversely affect the control performance in a significant way. The so called "control spillover" and instability of the control system were not observed. For example, the comparison between the experimental results of the instantaneous optimal control with time delay (see Fig. 4.10) and without time delay (see Fig. 4.9) showed little difference in the response behavior. This suggests that neglecting the time delay does not degrade the control effectiveness considerably.

2. The time interval of control implementation can be relatively long, as mentioned before.

3. The feedback control signal obtained from the instantaneous optimal control algorithm is not a function of the system parameters, as shown in Eqs. 2.23 and 2.30. Hence, the control efficiency in this case is not affected by paramenter variations.

SECTION 6

CONCLUSIONS

A systematic study on a hybrid sliding seismic isolation system using friction controllable bearings has been presented, including the following aspects:

1. A hybrid isolation system using friction controllable sliding bearings has been proposed for controlling response of a structure subjected earthquakes ranging from small to large intensities.

   This hybrid isolation system also has the following general advantage: the system requires smaller amounts of energy and power than the corresponding actuator-controlled system, and as a consequence, the use of accumulators for the source of energy is possible, thus eliminating the necessity of an emergency energy supply system.

2. Control algorithms, instantaneous optimal control and bang-bang control have been developed for controlling the friction force in the hybrid sliding isolation system. Standard control theory is difficult to apply in a straightforward fashion, in this case where the control force has a nonlinear feature.

3. A prototype hybrid sliding isolation system using friction controllable bearings has been physically developed, and shaking table experiments were performed on a rigid structural model equipped with such a hybrid system. A computer code has been developed for real-time on-line control implementation. The dynamic characteristics of the control system between bearing pressure and sliding friction have been identified. The results of hybrid sliding isolation experiments were compared with those of passive isolation.

4. Computer codes for the simulation of structural response under passive or hybrid control have been developed, and simulation analysis has been performed. The numerical results have been compared with experimental results.

Through the experimental and analytical study, the following conclusions have been obtained:

1. Significant advantage of the proposed hybrid sliding isolation system has been demonstrated: (1) for the small to medium earthquakes, the friction is controlled to make the structure slide easily to reduce the transfer of the seismic force to the structure to a minimum; (2) As the input earthquake becomes more intense, the friction is controlled to confine the sliding displacement of the structure to an acceptable range, while at the same time to keep the transfer of seismic force as small as possible. Such intelligent features of the friction controllable hybrid system does make the conventional passive sliding isolation system effective for all intensities of earthqukes.

2. Control algorithms developed for control of nonlinear friction force proved to be effective in achieving the desired control performances. In addition, they are practical and

easy for real-time on-line control operations.

3. The analytical model of dynamic characteristics between the bearing pressure control signal and the friction on the sliding interface has been identified. Computer simulation results excellently match the experiments. This implies that the analytical model represents the actual system very well, showing the possibility of utilizing the model to perform analytical study on other types of real structures equipped with the hybrid isolation system under different earthquake conditions.

4. The hybrid sliding isolation system appears to be quite robust, demonstrating the high potential for the application of the system to actual structures.

In the immediate future, possible implementation of the hybrid sliding isolation system to existing full-size structures such as buildings and girder bridges will be explored.

SECTION 7

REFERENCES

[1] Feng, Q., Fujii, S., Shinozuka, M., and Fujita, T., "Hybrid isolation system using friction-controllable sliding bearings," *Eighth VPI&SU Symposium on Dynamics and Large Structures,* Blacksburg, VA, 1991.

[2] Feng, Q., Shinozuka, M., Fujii, S., and Fujita, T., "A Hybrid isolation system for bridges," *Proceedings the First US-Japan Workshop on Earthquake Protective Systems for Bridges,* Buffalo, NY, 1991.

[3] Zayas, V., Stanley, L., Bozzo, L., and Mahin, S. A., "Feasibility and performance studies on improving the earthquake resistance of new and existing buildings using the friction pendulum system," *Report No. UCB/EERC-89/09,* Earthquake Engineering Research Center, UC, Berkeley, CA, 1989.

[4] Kawamura, S., Kitazawa, K., Hisano, M., and Nagashima, I., "Study of a sliding-type base isolation system. System conposition and element properties," *Proceedings of 9th World Conference on Earthquake Engineering,* Tokyo, Japan, 1988.

[5] Mostaghel, N. and Khodaverdian, M., "Dynamics of resilient friction base isolator (R-FBI)," *Earthquake Engineering and Structural Dynamics,* Vol. 15, No. 3, pp. 379-390, 1987.

[6] Constantinou. M. C., Mokha, A. S., and Reinhorn, A. M., "Experimental and analytical study of a combined silding disc bearing and helical steel spring isolation system," *Technical Report NCEER-90-0019,* NCEER, SUNY, Buffalo, NY, 1990.

[7] Constantinou. M. C., Mokha, A. S., and Reinhorn, A. M., "Study of sliding bearing and helical-steel-spring isolation system," *Journal of Structural Engineering,* ASCE, Vol. 117, No. 4. pp. 1257-1275, 1991.

[8] Fujita, T., Kabeya, K., and Hayamizu, Y., "Foundamental study of seismic isolation systems using semi-active control by variable dampers," *Seisan-kenkyu* , University of Tokyo, Vol. 41, No. 8, pp. 29-32, 1989. (in Japanese)

[9] Fujita, T., Kabeya, K., Hayamizu, Y., Aizawa, S., Higashino, M., Kubo, T., Haniuda, N., and Mori, T., "Semi-active seismic isolation system using controllable friction damper (1st report, development of controllable friction damper and fundamental strudy of semi-active control system)," *Journal of the Japan Society of the Japan Society of Mechanical Engineers,* C, Vol. 57, No. 536, pp. 29-32, 1991. (in Japanese)

[10] Feng, Q., and Shinozuka, M., "Use of a variable damper for hybrid control of bridge response under earthquake," *Proceedings of U.S. Natinal Workshop on Structural Control Research,* Los Angeles, CA, pp. 107-112, 1990.

[11] Feng, Q., and Shinozuka, M., "Control of seismic response of bridge structures by using variable dampers," *Journal of Intelligent Material Systems and Structures,* 1992 (accepted for publication)

[12] Yang, J.N., Long, F. X., and Wong, D., "Optimal control of nonlinear flexible structure," *Technical Report NCEER-88-0002,*, NCEER, SUNY, Buffalo, NY, 1988.

[13] Yang, J.N., Long, F. X., and Wong, D., "Optimal control of nonlinear structure," *Journal of Applied Mechanics,* Vol. 110, pp. 931-938, 1988.

[14] Fan, F-G., et al., "Base isolation of a multi-story building under a harmonic ground motion - a comparison of performances of various systems," *Technical Report NCEER-88-0002,* NCEER, SUNY, Buffalo, NY, 1988.

[15] Papalambros, P.Y. and Wilde, D.J., *Principles of optimal design,* Chapter 3, Cambridge University Press, Cambridge, 1988.

[16] Yang, J.N., et al., "Optimal hybrid control of seismic-excited nonlinear and inelastic structures," *International Workshop/Seminar on Intelligent Systems,* Perugia, Italy, June 27-29, 1991.

[17] Fujita, T., Feng, Q., Takenaka, E., Takano, T., and Suizu, Y., "Active isolation of sensitive equipment for weak earthquakes," *Proceedings of the 9th World Conference on Earthquake Engineering* , Tokyo and Kyoto, Japan, Vol VIII, pp. 459-464, 1988.

[18] Fujita, T., Feng, Q., Omi, T., and Suizu, Y., "An active isolation device using electric-hydraulic actuators for weak earthquakes," *Proc. of ASME Pressure Vessels and Piping Conference,* Honolulu, Hawaii, Vol. 181, pp. 95-99, 1989b.

[19] Fujita, T., Miyano, H, "On the performance of a tuned mass damper using xy-motion mechanism for vibration control in tall buildings," *Seisan-kenkyu* , University of Tokyo, Vol. 42, No. 12, pp. 681-683, 1990b. (in Japanese)

NATIONAL CENTER FOR EARTHQUAKE ENGINEERING RESEARCH
LIST OF TECHNICAL REPORTS

The National Center for Earthquake Engineering Research (NCEER) publishes technical reports on a variety of subjects related to earthquake engineering written by authors funded through NCEER. These reports are available from both NCEER's Publications Department and the National Technical Information Service (NTIS). Requests for reports should be directed to the Publications Department, National Center for Earthquake Engineering Research, State University of New York at Buffalo, Red Jacket Quadrangle, Buffalo, New York 14261. Reports can also be requested through NTIS, 5285 Port Royal Road, Springfield, Virginia 22161. NTIS accession numbers are shown in parenthesis, if available.

NCEER-87-0001 "First-Year Program in Research, Education and Technology Transfer," 3/5/87, (PB88-134275/AS).

NCEER-87-0002 "Experimental Evaluation of Instantaneous Optimal Algorithms for Structural Control," by R.C. Lin, T.T. Soong and A.M. Reinhorn, 4/20/87, (PB88-134341/AS).

NCEER-87-0003 "Experimentation Using the Earthquake Simulation Facilities at University at Buffalo," by A.M. Reinhorn and R.L. Ketter, to be published.

NCEER-87-0004 "The System Characteristics and Performance of a Shaking Table," by J.S. Hwang, K.C. Chang and G.C. Lee, 6/1/87, (PB88-134259/AS). This report is available only through NTIS (see address given above).

NCEER-87-0005 "A Finite Element Formulation for Nonlinear Viscoplastic Material Using a Q Model," by O. Gyebi and G. Dasgupta, 11/2/87, (PB88-213764/AS).

NCEER-87-0006 "Symbolic Manipulation Program (SMP) - Algebraic Codes for Two and Three Dimensional Finite Element Formulations," by X. Lee and G. Dasgupta, 11/9/87, (PB88-219522/AS).

NCEER-87-0007 "Instantaneous Optimal Control Laws for Tall Buildings Under Seismic Excitations," by J.N. Yang, A. Akbarpour and P. Ghaemmaghami, 6/10/87, (PB88-134333/AS).

NCEER-87-0008 "IDARC: Inelastic Damage Analysis of Reinforced Concrete Frame - Shear-Wall Structures," by Y.J. Park, A.M. Reinhorn and S.K. Kunnath, 7/20/87, (PB88-134325/AS).

NCEER-87-0009 "Liquefaction Potential for New York State: A Preliminary Report on Sites in Manhattan and Buffalo," by M. Budhu, V. Vijayakumar, R.F. Giese and L. Baumgras, 8/31/87, (PB88-163704/AS). This report is available only through NTIS (see address given above).

NCEER-87-0010 "Vertical and Torsional Vibration of Foundations in Inhomogeneous Media," by A.S. Veletsos and K.W. Dotson, 6/1/87, (PB88-134291/AS).

NCEER-87-0011 "Seismic Probabilistic Risk Assessment and Seismic Margins Studies for Nuclear Power Plants," by Howard H.M. Hwang, 6/15/87, (PB88-134267/AS).

NCEER-87-0012 "Parametric Studies of Frequency Response of Secondary Systems Under Ground-Acceleration Excitations," by Y. Yong and Y.K. Lin, 6/10/87, (PB88-134309/AS).

NCEER-87-0013 "Frequency Response of Secondary Systems Under Seismic Excitation," by J.A. HoLung, J. Cai and Y.K. Lin, 7/31/87, (PB88-134317/AS).

NCEER-87-0014 "Modelling Earthquake Ground Motions in Seismically Active Regions Using Parametric Time Series Methods," by G.W. Ellis and A.S. Cakmak, 8/25/87, (PB88-134283/AS).

NCEER-87-0015 "Detection and Assessment of Seismic Structural Damage," by E. DiPasquale and A.S. Cakmak, 8/25/87, (PB88-163712/AS).

NCEER-87-0016 "Pipeline Experiment at Parkfield, California," by J. Isenberg and E. Richardson, 9/15/87, (PB88-163720/AS). This report is available only through NTIS (see address given above).

NCEER-87-0017 "Digital Simulation of Seismic Ground Motion," by M. Shinozuka, G. Deodatis and T. Harada, 8/31/87, (PB88-155197/AS). This report is available only through NTIS (see address given above).

NCEER-87-0018 "Practical Considerations for Structural Control: System Uncertainty, System Time Delay and Truncation of Small Control Forces," J.N. Yang and A. Akbarpour, 8/10/87, (PB88-163738/AS).

NCEER-87-0019 "Modal Analysis of Nonclassically Damped Structural Systems Using Canonical Transformation," by J.N. Yang, S. Sarkani and F.X. Long, 9/27/87, (PB88-187851/AS).

NCEER-87-0020 "A Nonstationary Solution in Random Vibration Theory," by J.R. Red-Horse and P.D. Spanos, 11/3/87, (PB88-163746/AS).

NCEER-87-0021 "Horizontal Impedances for Radially Inhomogeneous Viscoelastic Soil Layers," by A.S. Veletsos and K.W. Dotson, 10/15/87, (PB88-150859/AS).

NCEER-87-0022 "Seismic Damage Assessment of Reinforced Concrete Members," by Y.S. Chung, C. Meyer and M. Shinozuka, 10/9/87, (PB88-150867/AS). This report is available only through NTIS (see address given above).

NCEER-87-0023 "Active Structural Control in Civil Engineering," by T.T. Soong, 11/11/87, (PB88-187778/AS).

NCEER-87-0024 "Vertical and Torsional Impedances for Radially Inhomogeneous Viscoelastic Soil Layers," by K.W. Dotson and A.S. Veletsos, 12/87, (PB88-187786/AS).

NCEER-87-0025 "Proceedings from the Symposium on Seismic Hazards, Ground Motions, Soil-Liquefaction and Engineering Practice in Eastern North America," October 20-22, 1987, edited by K.H. Jacob, 12/87, (PB88-188115/AS).

NCEER-87-0026 "Report on the Whittier-Narrows, California, Earthquake of October 1, 1987," by J. Pantelic and A. Reinhorn, 11/87, (PB88-187752/AS). This report is available only through NTIS (see address given above).

NCEER-87-0027 "Design of a Modular Program for Transient Nonlinear Analysis of Large 3-D Building Structures," by S. Srivastav and J.F. Abel, 12/30/87, (PB88-187950/AS).

NCEER-87-0028 "Second-Year Program in Research, Education and Technology Transfer," 3/8/88, (PB88-219480/AS).

NCEER-88-0001 "Workshop on Seismic Computer Analysis and Design of Buildings With Interactive Graphics," by W. McGuire, J.F. Abel and C.H. Conley, 1/18/88, (PB88-187760/AS).

NCEER-88-0002 "Optimal Control of Nonlinear Flexible Structures," by J.N. Yang, F.X. Long and D. Wong, 1/22/88, (PB88-213772/AS).

NCEER-88-0003 "Substructuring Techniques in the Time Domain for Primary-Secondary Structural Systems," by G.D. Manolis and G. Juhn, 2/10/88, (PB88-213780/AS).

NCEER-88-0004 "Iterative Seismic Analysis of Primary-Secondary Systems," by A. Singhal, L.D. Lutes and P.D. Spanos, 2/23/88, (PB88-213798/AS).

NCEER-88-0005 "Stochastic Finite Element Expansion for Random Media," by P.D. Spanos and R. Ghanem, 3/14/88, (PB88-213806/AS).

NCEER-88-0006 "Combining Structural Optimization and Structural Control," by F.Y. Cheng and C.P. Pantelides, 1/10/88, (PB88-213814/AS).

NCEER-88-0007 "Seismic Performance Assessment of Code-Designed Structures," by H.H-M. Hwang, J-W. Jaw and H-J. Shau, 3/20/88, (PB88-219423/AS).

NCEER-88-0008 "Reliability Analysis of Code-Designed Structures Under Natural Hazards," by H.H-M. Hwang, H. Ushiba and M. Shinozuka, 2/29/88, (PB88-229471/AS).

NCEER-88-0009 "Seismic Fragility Analysis of Shear Wall Structures," by J-W Jaw and H.H-M. Hwang, 4/30/88, (PB89-102867/AS).

NCEER-88-0010 "Base Isolation of a Multi-Story Building Under a Harmonic Ground Motion - A Comparison of Performances of Various Systems," by F-G Fan, G. Ahmadi and I.G. Tadjbakhsh, 5/18/88, (PB89-122238/AS).

NCEER-88-0011 "Seismic Floor Response Spectra for a Combined System by Green's Functions," by F.M. Lavelle, L.A. Bergman and P.D. Spanos, 5/1/88, (PB89-102875/AS).

NCEER-88-0012 "A New Solution Technique for Randomly Excited Hysteretic Structures," by G.Q. Cai and Y.K. Lin, 5/16/88, (PB89-102883/AS).

NCEER-88-0013 "A Study of Radiation Damping and Soil-Structure Interaction Effects in the Centrifuge," by K. Weissman, supervised by J.H. Prevost, 5/24/88, (PB89-144703/AS).

NCEER-88-0014 "Parameter Identification and Implementation of a Kinematic Plasticity Model for Frictional Soils," by J.H. Prevost and D.V. Griffiths, to be published.

NCEER-88-0015 "Two- and Three- Dimensional Dynamic Finite Element Analyses of the Long Valley Dam," by D.V. Griffiths and J.H. Prevost, 6/17/88, (PB89-144711/AS).

NCEER-88-0016 "Damage Assessment of Reinforced Concrete Structures in Eastern United States," by A.M. Reinhorn, M.J. Seidel, S.K. Kunnath and Y.J. Park, 6/15/88, (PB89-122220/AS).

NCEER-88-0017 "Dynamic Compliance of Vertically Loaded Strip Foundations in Multilayered Viscoelastic Soils," by S. Ahmad and A.S.M. Israil, 6/17/88, (PB89-102891/AS).

NCEER-88-0018 "An Experimental Study of Seismic Structural Response With Added Viscoelastic Dampers," by R.C. Lin, Z. Liang, T.T. Soong and R.H. Zhang, 6/30/88, (PB89-122212/AS). This report is available only through NTIS (see address given above).

NCEER-88-0019 "Experimental Investigation of Primary - Secondary System Interaction," by G.D. Manolis, G. Juhn and A.M. Reinhorn, 5/27/88, (PB89-122204/AS).

NCEER-88-0020 "A Response Spectrum Approach For Analysis of Nonclassically Damped Structures," by J.N. Yang, S. Sarkani and F.X. Long, 4/22/88, (PB89-102909/AS).

NCEER-88-0021 "Seismic Interaction of Structures and Soils: Stochastic Approach," by A.S. Veletsos and A.M. Prasad, 7/21/88, (PB89-122196/AS).

NCEER-88-0022 "Identification of the Serviceability Limit State and Detection of Seismic Structural Damage," by E. DiPasquale and A.S. Cakmak, 6/15/88, (PB89-122188/AS). This report is available only through NTIS (see address given above).

NCEER-88-0023 "Multi-Hazard Risk Analysis: Case of a Simple Offshore Structure," by B.K. Bhartia and E.H. Vanmarcke, 7/21/88, (PB89-145213/AS).

NCEER-88-0024 "Automated Seismic Design of Reinforced Concrete Buildings," by Y.S. Chung, C. Meyer and M. Shinozuka, 7/5/88, (PB89-122170/AS). This report is available only through NTIS (see address given above).

NCEER-88-0025 "Experimental Study of Active Control of MDOF Structures Under Seismic Excitations," by L.L. Chung, R.C. Lin, T.T. Soong and A.M. Reinhorn, 7/10/88, (PB89-122600/AS).

NCEER-88-0026 "Earthquake Simulation Tests of a Low-Rise Metal Structure," by J.S. Hwang, K.C. Chang, G.C. Lee and R.L. Ketter, 8/1/88, (PB89-102917/AS).

NCEER-88-0027 "Systems Study of Urban Response and Reconstruction Due to Catastrophic Earthquakes," by F. Kozin and H.K. Zhou, 9/22/88, (PB90-162348/AS).

NCEER-88-0028 "Seismic Fragility Analysis of Plane Frame Structures," by H.H-M. Hwang and Y.K. Low, 7/31/88, (PB89-131445/AS).

NCEER-88-0029 "Response Analysis of Stochastic Structures," by A. Kardara, C. Bucher and M. Shinozuka, 9/22/88, (PB89-174429/AS).

NCEER-88-0030 "Nonnormal Accelerations Due to Yielding in a Primary Structure," by D.C.K. Chen and L.D. Lutes, 9/19/88, (PB89-131437/AS).

NCEER-88-0031 "Design Approaches for Soil-Structure Interaction," by A.S. Veletsos, A.M. Prasad and Y. Tang, 12/30/88, (PB89-174437/AS). This report is available only through NTIS (see address given above).

NCEER-88-0032 "A Re-evaluation of Design Spectra for Seismic Damage Control," by C.J. Turkstra and A.G. Tallin, 11/7/88, (PB89-145221/AS).

NCEER-88-0033 "The Behavior and Design of Noncontact Lap Splices Subjected to Repeated Inelastic Tensile Loading," by V.E. Sagan, P. Gergely and R.N. White, 12/8/88, (PB89-163737/AS).

NCEER-88-0034 "Seismic Response of Pile Foundations," by S.M. Mamoon, P.K. Banerjee and S. Ahmad, 11/1/88, (PB89-145239/AS).

NCEER-88-0035 "Modeling of R/C Building Structures With Flexible Floor Diaphragms (IDARC2)," by A.M. Reinhorn, S.K. Kunnath and N. Panahshahi, 9/7/88, (PB89-207153/AS).

NCEER-88-0036 "Solution of the Dam-Reservoir Interaction Problem Using a Combination of FEM, BEM with Particular Integrals, Modal Analysis, and Substructuring," by C-S. Tsai, G.C. Lee and R.L. Ketter, 12/31/88, (PB89-207146/AS).

NCEER-88-0037 "Optimal Placement of Actuators for Structural Control," by F.Y. Cheng and C.P. Pantelides, 8/15/88, (PB89-162846/AS).

NCEER-88-0038 "Teflon Bearings in Aseismic Base Isolation: Experimental Studies and Mathematical Modeling," by A. Mokha, M.C. Constantinou and A.M. Reinhorn, 12/5/88, (PB89-218457/AS). This report is available only through NTIS (see address given above).

NCEER-88-0039 "Seismic Behavior of Flat Slab High-Rise Buildings in the New York City Area," by P. Weidlinger and M. Ettouney, 10/15/88, (PB90-145681/AS).

NCEER-88-0040 "Evaluation of the Earthquake Resistance of Existing Buildings in New York City," by P. Weidlinger and M. Ettouney, 10/15/88, to be published.

NCEER-88-0041 "Small-Scale Modeling Techniques for Reinforced Concrete Structures Subjected to Seismic Loads," by W. Kim, A. El-Attar and R.N. White, 11/22/88, (PB89-189625/AS).

NCEER-88-0042 "Modeling Strong Ground Motion from Multiple Event Earthquakes," by G.W. Ellis and A.S. Cakmak, 10/15/88, (PB89-174445/AS).

NCEER-88-0043 "Nonstationary Models of Seismic Ground Acceleration," by M. Grigoriu, S.E. Ruiz and E. Rosenblueth, 7/15/88, (PB89-189617/AS).

NCEER-88-0044 "SARCF User's Guide: Seismic Analysis of Reinforced Concrete Frames," by Y.S. Chung, C. Meyer and M. Shinozuka, 11/9/88, (PB89-174452/AS).

NCEER-88-0045 "First Expert Panel Meeting on Disaster Research and Planning," edited by J. Pantelic and J. Stoyle, 9/15/88, (PB89-174460/AS).

NCEER-88-0046 "Preliminary Studies of the Effect of Degrading Infill Walls on the Nonlinear Seismic Response of Steel Frames," by C.Z. Chrysostomou, P. Gergely and J.F. Abel, 12/19/88, (PB89-208383/AS).

NCEER-88-0047 "Reinforced Concrete Frame Component Testing Facility - Design, Construction, Instrumentation and Operation," by S.P. Pessiki, C. Conley, T. Bond, P. Gergely and R.N. White, 12/16/88, (PB89-174478/AS).

NCEER-89-0001 "Effects of Protective Cushion and Soil Compliancy on the Response of Equipment Within a Seismically Excited Building," by J.A. HoLung, 2/16/89, (PB89-207179/AS).

NCEER-89-0002 "Statistical Evaluation of Response Modification Factors for Reinforced Concrete Structures," by H.H-M. Hwang and J-W. Jaw, 2/17/89, (PB89-207187/AS).

NCEER-89-0003 "Hysteretic Columns Under Random Excitation," by G-Q. Cai and Y.K. Lin, 1/9/89, (PB89-196513/AS).

NCEER-89-0004 "Experimental Study of 'Elephant Foot Bulge' Instability of Thin-Walled Metal Tanks," by Z-H. Jia and R.L. Ketter, 2/22/89, (PB89-207195/AS).

NCEER-89-0005 "Experiment on Performance of Buried Pipelines Across San Andreas Fault," by J. Isenberg, E. Richardson and T.D. O'Rourke, 3/10/89, (PB89-218440/AS).

NCEER-89-0006 "A Knowledge-Based Approach to Structural Design of Earthquake-Resistant Buildings," by M. Subramani, P. Gergely, C.H. Conley, J.F. Abel and A.H. Zaghw, 1/15/89, (PB89-218465/AS).

NCEER-89-0007 "Liquefaction Hazards and Their Effects on Buried Pipelines," by T.D. O'Rourke and P.A. Lane, 2/1/89, (PB89-218481).

NCEER-89-0008 "Fundamentals of System Identification in Structural Dynamics," by H. Imai, C-B. Yun, O. Maruyama and M. Shinozuka, 1/26/89, (PB89-207211/AS).

NCEER-89-0009 "Effects of the 1985 Michoacan Earthquake on Water Systems and Other Buried Lifelines in Mexico," by A.G. Ayala and M.J. O'Rourke, 3/8/89, (PB89-207229/AS).

NCEER-89-R010 "NCEER Bibliography of Earthquake Education Materials," by K.E.K. Ross, Second Revision, 9/1/89, (PB90-125352/AS).

NCEER-89-0011 "Inelastic Three-Dimensional Response Analysis of Reinforced Concrete Building Structures (IDARC-3D), Part I - Modeling," by S.K. Kunnath and A.M. Reinhorn, 4/17/89, (PB90-114612/AS).

NCEER-89-0012 "Recommended Modifications to ATC-14," by C.D. Poland and J.O. Malley, 4/12/89, (PB90-108648/AS).

NCEER-89-0013 "Repair and Strengthening of Beam-to-Column Connections Subjected to Earthquake Loading," by M. Corazao and A.J. Durrani, 2/28/89, (PB90-109885/AS).

NCEER-89-0014 "Program EXKAL2 for Identification of Structural Dynamic Systems," by O. Maruyama, C-B. Yun, M. Hoshiya and M. Shinozuka, 5/19/89, (PB90-109877/AS).

NCEER-89-0015 "Response of Frames With Bolted Semi-Rigid Connections, Part I - Experimental Study and Analytical Predictions," by P.J. DiCorso, A.M. Reinhorn, J.R. Dickerson, J.B. Radziminski and W.L. Harper, 6/1/89, to be published.

NCEER-89-0016 "ARMA Monte Carlo Simulation in Probabilistic Structural Analysis," by P.D. Spanos and M.P. Mignolet, 7/10/89, (PB90-109893/AS).

NCEER-89-P017 "Preliminary Proceedings from the Conference on Disaster Preparedness - The Place of Earthquake Education in Our Schools," Edited by K.E.K. Ross, 6/23/89.

NCEER-89-0017 "Proceedings from the Conference on Disaster Preparedness - The Place of Earthquake Education in Our Schools," Edited by K.E.K. Ross, 12/31/89, (PB90-207895). This report is available only through NTIS (see address given above).

NCEER-89-0018 "Multidimensional Models of Hysteretic Material Behavior for Vibration Analysis of Shape Memory Energy Absorbing Devices, by E.J. Graesser and F.A. Cozzarelli, 6/7/89, (PB90-164146/AS).

NCEER-89-0019 "Nonlinear Dynamic Analysis of Three-Dimensional Base Isolated Structures (3D-BASIS)," by S. Nagarajaiah, A.M. Reinhorn and M.C. Constantinou, 8/3/89, (PB90-161936/AS). This report is available only through NTIS (see address given above).

NCEER-89-0020 "Structural Control Considering Time-Rate of Control Forces and Control Rate Constraints," by F.Y. Cheng and C.P. Pantelides, 8/3/89, (PB90-120445/AS).

NCEER-89-0021 "Subsurface Conditions of Memphis and Shelby County," by K.W. Ng, T-S. Chang and H-H.M. Hwang, 7/26/89, (PB90-120437/AS).

NCEER-89-0022 "Seismic Wave Propagation Effects on Straight Jointed Buried Pipelines," by K. Elhmadi and M.J. O'Rourke, 8/24/89, (PB90-162322/AS).

NCEER-89-0023 "Workshop on Serviceability Analysis of Water Delivery Systems," edited by M. Grigoriu, 3/6/89, (PB90-127424/AS).

NCEER-89-0024 "Shaking Table Study of a 1/5 Scale Steel Frame Composed of Tapered Members," by K.C. Chang, J.S. Hwang and G.C. Lee, 9/18/89, (PB90-160169/AS).

NCEER-89-0025 "DYNA1D: A Computer Program for Nonlinear Seismic Site Response Analysis - Technical Documentation," by Jean H. Prevost, 9/14/89, (PB90-161944/AS). This report is available only through NTIS (see address given above).

NCEER-89-0026 "1:4 Scale Model Studies of Active Tendon Systems and Active Mass Dampers for Aseismic Protection," by A.M. Reinhorn, T.T. Soong, R.C. Lin, Y.P. Yang, Y. Fukao, H. Abe and M. Nakai, 9/15/89, (PB90-173246/AS).

NCEER-89-0027 "Scattering of Waves by Inclusions in a Nonhomogeneous Elastic Half Space Solved by Boundary Element Methods," by P.K. Hadley, A. Askar and A.S. Cakmak, 6/15/89, (PB90-145699/AS).

NCEER-89-0028 "Statistical Evaluation of Deflection Amplification Factors for Reinforced Concrete Structures," by H.H.M. Hwang, J-W. Jaw and A.L. Ch'ng, 8/31/89, (PB90-164633/AS).

NCEER-89-0029 "Bedrock Accelerations in Memphis Area Due to Large New Madrid Earthquakes," by H.H.M. Hwang, C.H.S. Chen and G. Yu, 11/7/89, (PB90-162330/AS).

NCEER-89-0030 "Seismic Behavior and Response Sensitivity of Secondary Structural Systems," by Y.Q. Chen and T.T. Soong, 10/23/89, (PB90-164658/AS).

NCEER-89-0031 "Random Vibration and Reliability Analysis of Primary-Secondary Structural Systems," by Y. Ibrahim, M. Grigoriu and T.T. Soong, 11/10/89, (PB90-161951/AS).

NCEER-89-0032 "Proceedings from the Second U.S. - Japan Workshop on Liquefaction, Large Ground Deformation and Their Effects on Lifelines, September 26-29, 1989," Edited by T.D. O'Rourke and M. Hamada, 12/1/89, (PB90-209388/AS).

NCEER-89-0033 "Deterministic Model for Seismic Damage Evaluation of Reinforced Concrete Structures," by J.M. Bracci, A.M. Reinhorn, J.B. Mander and S.K. Kunnath, 9/27/89.

NCEER-89-0034 "On the Relation Between Local and Global Damage Indices," by E. DiPasquale and A.S. Cakmak, 8/15/89, (PB90-173865).

NCEER-89-0035 "Cyclic Undrained Behavior of Nonplastic and Low Plasticity Silts," by A.J. Walker and H.E. Stewart, 7/26/89, (PB90-183518/AS).

NCEER-89-0036 "Liquefaction Potential of Surficial Deposits in the City of Buffalo, New York," by M. Budhu, R. Giese and L. Baumgrass, 1/17/89, (PB90-208455/AS).

NCEER-89-0037 "A Deterministic Assessment of Effects of Ground Motion Incoherence," by A.S. Veletsos and Y. Tang, 7/15/89, (PB90-164294/AS).

NCEER-89-0038 "Workshop on Ground Motion Parameters for Seismic Hazard Mapping," July 17-18, 1989, edited by R.V. Whitman, 12/1/89, (PB90-173923/AS).

NCEER-89-0039 "Seismic Effects on Elevated Transit Lines of the New York City Transit Authority," by C.J. Costantino, C.A. Miller and E. Heymsfield, 12/26/89, (PB90-207887/AS).

NCEER-89-0040 "Centrifugal Modeling of Dynamic Soil-Structure Interaction," by K. Weissman, Supervised by J.H. Prevost, 5/10/89, (PB90-207879/AS).

NCEER-89-0041 "Linearized Identification of Buildings With Cores for Seismic Vulnerability Assessment," by I-K. Ho and A.E. Aktan, 11/1/89, (PB90-251943/AS).

NCEER-90-0001 "Geotechnical and Lifeline Aspects of the October 17, 1989 Loma Prieta Earthquake in San Francisco," by T.D. O'Rourke, H.E. Stewart, F.T. Blackburn and T.S. Dickerman, 1/90, (PB90-208596/AS).

NCEER-90-0002 "Nonnormal Secondary Response Due to Yielding in a Primary Structure," by D.C.K. Chen and L.D. Lutes, 2/28/90, (PB90-251976/AS).

NCEER-90-0003 "Earthquake Education Materials for Grades K-12," by K.E.K. Ross, 4/16/90, (PB91-113415/AS).

NCEER-90-0004 "Catalog of Strong Motion Stations in Eastern North America," by R.W. Busby, 4/3/90, (PB90-251984)/AS.

NCEER-90-0005 "NCEER Strong-Motion Data Base: A User Manual for the GeoBase Release (Version 1.0 for the Sun3)," by P. Friberg and K. Jacob, 3/31/90 (PB90-258062/AS).

NCEER-90-0006 "Seismic Hazard Along a Crude Oil Pipeline in the Event of an 1811-1812 Type New Madrid Earthquake," by H.H.M. Hwang and C-H.S. Chen, 4/16/90(PB90-258054).

NCEER-90-0007 "Site-Specific Response Spectra for Memphis Sheahan Pumping Station," by H.H.M. Hwang and C.S. Lee, 5/15/90, (PB91-108811/AS).

NCEER-90-0008 "Pilot Study on Seismic Vulnerability of Crude Oil Transmission Systems," by T. Ariman, R. Dobry, M. Grigoriu, F. Kozin, M. O'Rourke, T. O'Rourke and M. Shinozuka, 5/25/90, (PB91-108837/AS).

NCEER-90-0009 "A Program to Generate Site Dependent Time Histories: EQGEN," by G.W. Ellis, M. Srinivasan and A.S. Cakmak, 1/30/90, (PB91-108829/AS).

NCEER-90-0010 "Active Isolation for Seismic Protection of Operating Rooms," by M.E. Talbott, Supervised by M. Shinozuka, 6/8/9, (PB91-110205/AS).

NCEER-90-0011 "Program LINEARID for Identification of Linear Structural Dynamic Systems," by C-B. Yun and M. Shinozuka, 6/25/90, (PB91-110312/AS).

NCEER-90-0012 "Two-Dimensional Two-Phase Elasto-Plastic Seismic Response of Earth Dams," by A.N. Yiagos, Supervised by J.H. Prevost, 6/20/90, (PB91-110197/AS).

NCEER-90-0013 "Secondary Systems in Base-Isolated Structures: Experimental Investigation, Stochastic Response and Stochastic Sensitivity," by G.D. Manolis, G. Juhn, M.C. Constantinou and A.M. Reinhorn, 7/1/90, (PB91-110320/AS).

NCEER-90-0014 "Seismic Behavior of Lightly-Reinforced Concrete Column and Beam-Column Joint Details," by S.P. Pessiki, C.H. Conley, P. Gergely and R.N. White, 8/22/90, (PB91-108795/AS).

NCEER-90-0015 "Two Hybrid Control Systems for Building Structures Under Strong Earthquakes," by J.N. Yang and A. Danielians, 6/29/90, (PB91-125393/AS).

NCEER-90-0016 "Instantaneous Optimal Control with Acceleration and Velocity Feedback," by J.N. Yang and Z. Li, 6/29/90, (PB91-125401/AS).

NCEER-90-0017 "Reconnaissance Report on the Northern Iran Earthquake of June 21, 1990," by M. Mehrain, 10/4/90, (PB91-125377/AS).

NCEER-90-0018 "Evaluation of Liquefaction Potential in Memphis and Shelby County," by T.S. Chang, P.S. Tang, C.S. Lee and H. Hwang, 8/10/90, (PB91-125427/AS).

NCEER-90-0019 "Experimental and Analytical Study of a Combined Sliding Disc Bearing and Helical Steel Spring Isolation System," by M.C. Constantinou, A.S. Mokha and A.M. Reinhorn, 10/4/90, (PB91-125385/AS).

NCEER-90-0020 "Experimental Study and Analytical Prediction of Earthquake Response of a Sliding Isolation System with a Spherical Surface," by A.S. Mokha, M.C. Constantinou and A.M. Reinhorn, 10/11/90, (PB91-125419/AS).

NCEER-90-0021 "Dynamic Interaction Factors for Floating Pile Groups," by G. Gazetas, K. Fan, A. Kaynia and E. Kausel, 9/10/90, (PB91-170381/AS).

NCEER-90-0022 "Evaluation of Seismic Damage Indices for Reinforced Concrete Structures," by S. Rodriguez-Gomez and A.S. Cakmak, 9/30/90, PB91-171322/AS).

NCEER-90-0023 "Study of Site Response at a Selected Memphis Site," by H. Desai, S. Ahmad, E.S. Gazetas and M.R. Oh, 10/11/90, (PB91-196857/AS).

NCEER-90-0024 "A User's Guide to Strongmo: Version 1.0 of NCEER's Strong-Motion Data Access Tool for PCs and Terminals," by P.A. Friberg and C.A.T. Susch, 11/15/90, (PB91-171272/AS).

NCEER-90-0025 "A Three-Dimensional Analytical Study of Spatial Variability of Seismic Ground Motions," by L-L. Hong and A.H.-S. Ang, 10/30/90, (PB91-170399/AS).

NCEER-90-0026 "MUMOID User's Guide - A Program for the Identification of Modal Parameters," by S. Rodriguez-Gomez and E. DiPasquale, 9/30/90, (PB91-171298/AS).

NCEER-90-0027 "SARCF-II User's Guide - Seismic Analysis of Reinforced Concrete Frames," by S. Rodriguez-Gomez, Y.S. Chung and C. Meyer, 9/30/90, (PB91-171280/AS).

NCEER-90-0028 "Viscous Dampers: Testing, Modeling and Application in Vibration and Seismic Isolation," by N. Makris and M.C. Constantinou, 12/20/90 (PB91-190561/AS).

NCEER-90-0029 "Soil Effects on Earthquake Ground Motions in the Memphis Area," by H. Hwang, C.S. Lee, K.W. Ng and T.S. Chang, 8/2/90, (PB91-190751/AS).

NCEER-91-0001 "Proceedings from the Third Japan-U.S. Workshop on Earthquake Resistant Design of Lifeline Facilities and Countermeasures for Soil Liquefaction, December 17-19, 1990," edited by T.D. O'Rourke and M. Hamada, 2/1/91, (PB91-179259/AS).

NCEER-91-0002 "Physical Space Solutions of Non-Proportionally Damped Systems," by M. Tong, Z. Liang and G.C. Lee, 1/15/91, (PB91-179242/AS).

NCEER-91-0003 "Seismic Response of Single Piles and Pile Groups," by K. Fan and G. Gazetas, 1/10/91, (PB92-174994/AS).

NCEER-91-0004 "Damping of Structures: Part 1 - Theory of Complex Damping," by Z. Liang and G. Lee, 10/10/91, (PB92-197235/AS).

NCEER-91-0005 "3D-BASIS - Nonlinear Dynamic Analysis of Three Dimensional Base Isolated Structures: Part II," by S. Nagarajaiah, A.M. Reinhorn and M.C. Constantinou, 2/28/91, (PB91-190553/AS).

NCEER-91-0006 "A Multidimensional Hysteretic Model for Plasticity Deforming Metals in Energy Absorbing Devices," by E.J. Graesser and F.A. Cozzarelli, 4/9/91, (PB92-108364/AS).

NCEER-91-0007 "A Framework for Customizable Knowledge-Based Expert Systems with an Application to a KBES for Evaluating the Seismic Resistance of Existing Buildings," by E.G. Ibarra-Anaya and S.J. Fenves, 4/9/91, (PB91-210930/AS).

NCEER-91-0008 "Nonlinear Analysis of Steel Frames with Semi-Rigid Connections Using the Capacity Spectrum Method," by G.G. Deierlein, S-H. Hsieh, Y-J. Shen and J.F. Abel, 7/2/91, (PB92-113828/AS).

NCEER-91-0009 "Earthquake Education Materials for Grades K-12," by K.E.K. Ross, 4/30/91, (PB91-212142/AS).

NCEER-91-0010 "Phase Wave Velocities and Displacement Phase Differences in a Harmonically Oscillating Pile," by N. Makris and G. Gazetas, 7/8/91, (PB92-108356/AS).

NCEER-91-0011 "Dynamic Characteristics of a Full-Size Five-Story Steel Structure and a 2/5 Scale Model," by K.C. Chang, G.C. Yao, G.C. Lee, D.S. Hao and Y.C. Yeh," 7/2/91.

NCEER-91-0012 "Seismic Response of a 2/5 Scale Steel Structure with Added Viscoelastic Dampers," by K.C. Chang, T.T. Soong, S-T. Oh and M.L. Lai, 5/17/91 (PB92-110816/AS).

NCEER-91-0013 "Earthquake Response of Retaining Walls; Full-Scale Testing and Computational Modeling," by S. Alampalli and A-W.M. Elgamal, 6/20/91, to be published.

NCEER-91-0014 "3D-BASIS-M: Nonlinear Dynamic Analysis of Multiple Building Base Isolated Structures," by P.C. Tsopelas, S. Nagarajaiah, M.C. Constantinou and A.M. Reinhorn, 5/28/91, (PB92-113885/AS).

NCEER-91-0015 "Evaluation of SEAOC Design Requirements for Sliding Isolated Structures," by D. Theodossiou and M.C. Constantinou, 6/10/91, (PB92-114602/AS).

NCEER-91-0016 "Closed-Loop Modal Testing of a 27-Story Reinforced Concrete Flat Plate-Core Building," by H.R. Somaprasad, T. Toksoy, H. Yoshiyuki and A.E. Aktan, 7/15/91, (PB92-129980/AS).

NCEER-91-0017 "Shake Table Test of a 1/6 Scale Two-Story Lightly Reinforced Concrete Building," by A.G. El-Attar, R.N. White and P. Gergely, 2/28/91, (PB92-222447/AS).

NCEER-91-0018 "Shake Table Test of a 1/8 Scale Three-Story Lightly Reinforced Concrete Building," by A.G. El-Attar, R.N. White and P. Gergely, 2/28/91.

NCEER-91-0019 "Transfer Functions for Rigid Rectangular Foundations," by A.S. Veletsos, A.M. Prasad and W.H. Wu, 7/31/91, to be published.

NCEER-91-0020 "Hybrid Control of Seismic-Excited Nonlinear and Inelastic Structural Systems," by J.N. Yang, Z. Li and A. Danielians, 8/1/91, (PB92-143171/AS).

NCEER-91-0021 "The NCEER-91 Earthquake Catalog: Improved Intensity-Based Magnitudes and Recurrence Relations for U.S. Earthquakes East of New Madrid," by L. Seeber and J.G. Armbruster, 8/28/91, (PB92-176742/AS).

NCEER-91-0022 "Proceedings from the Implementation of Earthquake Planning and Education in Schools: The Need for Change - The Roles of the Changemakers," by K.E.K. Ross and F. Winslow, 7/23/91, (PB92-129998/AS).

NCEER-91-0023 "A Study of Reliability-Based Criteria for Seismic Design of Reinforced Concrete Frame Buildings," by H.H.M. Hwang and H-M. Hsu, 8/10/91, (PB92-140235/AS).

NCEER-91-0024 "Experimental Verification of a Number of Structural System Identification Algorithms," by R.G. Ghanem, H. Gavin and M. Shinozuka, 9/18/91, (PB92-176577/AS).

NCEER-91-0025 "Probabilistic Evaluation of Liquefaction Potential," by H.H.M. Hwang and C.S. Lee," 11/25/91, (PB92-143429/AS).

NCEER-91-0026 "Instantaneous Optimal Control for Linear, Nonlinear and Hysteretic Structures - Stable Controllers," by J.N. Yang and Z. Li, 11/15/91, (PB92-163807/AS).

NCEER-91-0027 "Experimental and Theoretical Study of a Sliding Isolation System for Bridges," by M.C. Constantinou, A. Kartoum, A.M. Reinhorn and P. Bradford, 11/15/91, (PB92-176973/AS).

NCEER-92-0001 "Case Studies of Liquefaction and Lifeline Performance During Past Earthquakes, Volume 1: Japanese Case Studies," Edited by M. Hamada and T. O'Rourke, 2/17/92, (PB92-197243/AS).

NCEER-92-0002 "Case Studies of Liquefaction and Lifeline Performance During Past Earthquakes, Volume 2: United States Case Studies," Edited by T. O'Rourke and M. Hamada, 2/17/92, (PB92-197250/AS).

NCEER-92-0003 "Issues in Earthquake Education," Edited by K. Ross, 2/3/92, (PB92-222389/AS).

NCEER-92-0004 "Proceedings from the First U.S. - Japan Workshop on Earthquake Protective Systems for Bridges," 2/4/92, to be published.

NCEER-92-0005 "Seismic Ground Motion from a Haskell-Type Source in a Multiple-Layered Half-Space," A.P. Theoharis, G. Deodatis and M. Shinozuka, 1/2/92, to be published.

NCEER-92-0006 "Proceedings from the Site Effects Workshop," Edited by R. Whitman, 2/29/92, (PB92-197201/AS).

NCEER-92-0007 "Engineering Evaluation of Permanent Ground Deformations Due to Seismically-Induced Liquefaction," by M.H. Baziar, R. Dobry and A-W.M. Elgamal, 3/24/92, (PB92-222421/AS).

NCEER-92-0008 "A Procedure for the Seismic Evaluation of Buildings in the Central and Eastern United States," by C.D. Poland and J.O. Malley, 4/2/92, (PB92-222439/AS).

NCEER-92-0009 "Experimental and Analytical Study of a Hybrid Isolation System Using Friction Controllable Sliding Bearings," by M.Q. Feng, S. Fujii and M. Shinozuka, 5/15/92.